

1 Interfered Chromosome Pairing Promotes Meiosis 2 Instability of Autotetraploid Arabidopsis by High 3 Temperatures

4
5 Huiqi Fu^{1#}, Jiayi Zhao^{1#}, Ziming Ren^{2#}, Ke Yang¹, Chong Wang³, Xiaohong Zhang¹, Ibrahim
6 Eid Elesawi^{4, 5}, Xianhua Zhang⁶, Jing Xia¹, Chunli Chen^{4, 7}, Ping Lu⁸, Yongxing Chen⁸, Hong
7 Liu^{1✉}, Guanghui Yu^{1✉}, Bing Liu^{1✉*}

8 ¹College of Life Sciences, South-Central University for Nationalities, Wuhan 430074, China;

9 ²College of Agriculture and Biotechnology, Zhejiang University, Zhejiang 310058, China;

10 ³College of Life Sciences, Shanghai Normal University, Shanghai 200234, China;

11 ⁴College of Life Science and Technology, Huazhong Agricultural University, Wuhan, 430070;

12 ⁵Agricultural Biochemistry Department, Faculty of Agriculture, Zagazig University, Zagazig
13 44511, Egypt;

14 ⁶School of Life Sciences, Hubei University, Wuhan 430062, China;

15 ⁷Key Laboratory of Plant Resource Conservation and Germplasm Innovation in Mountainous
16 Region, College of Life Science, Guizhou University, Guiyang 550025, China;

17 ⁸State Key Laboratory of Plant Cell and Chromosome Engineering, Institute of Genetics and
18 Developmental Biology, Chinese Academy of Sciences, Beijing 100101, China

19 #These authors contributed equally to this work;

20 ✉Authors for communication:

21 Hong Liu (liuhong@mail.scuec.edu.cn);

22 Guanghui Yu (yusheen@163.com);

23 Bing Liu (bl472@scuec.edu.cn);

24 *Senior author: Bing Liu

25 Abstract

26
27 Alterations of environmental temperature affect multiple meiosis processes in flowering
28 plants. Polyploid plants derived from whole genome duplication (WGD) have enhanced
29 genetic plasticity and tolerance to environmental stress, but meanwhile face a challenge for
30 organization and segregation of doubled chromosome sets. In this study, we investigated the
31 impact of increased environmental temperature on male meiosis in autotetraploid *Arabidopsis*
32 *thaliana*. Under low to mildly-increased temperatures (5-28°C), irregular chromosome
33 segregation universally takes place in synthesized autotetraploid Columbia-0 (Col-0). Similar
34 meiosis lesions occur in autotetraploid rice (*Oryza sativa* L.) and allotetraploid canola
35 (*Brassica napus* cv. Westar), but not in evolutionary-derived hexaploid wheat (*Triticum*
36 *aestivum*). As temperature increases to extremely high, chromosome separation and tetrad
37 formation are severely disordered due to univalent formation caused by suppressed crossing-
38 over. We found a strong correlation between tetravalent formation and successful
39 chromosome pairing, both of which are negatively correlated with temperature elevation,
40 suggesting that increased temperature interferes with crossing-over prominently by impacting

41 homolog pairing. Besides, we showed that loading irregularities of axis proteins ASY1 and
42 ASY4 co-localize on the chromosomes of *syn1* mutant, and the heat-stressed diploid and
43 autotetraploid Col-0, revealing that heat stress affects lateral region of synaptonemal complex
44 (SC) by impacting stability of axis. Moreover, we showed that chromosome axis and SC in
45 autotetraploid Col-0 are more sensitive to increased temperature than that of diploid
46 *Arabidopsis*. Taken together, our study provide evidence suggesting that WGD without
47 evolutionary and/or natural adaption negatively affects stability and thermal tolerance of
48 meiotic recombination in *Arabidopsis thaliana*.

49

50 Introduction

51

52 Meiosis is a specialized type of cell division that, in plants, occurs in pollen mother cells
53 (PMCs) and/or megasporocytes giving rise to gametes with a halved ploidy. At early stages of
54 meiosis, meiotic recombination takes place between homologous chromosomes leading to
55 exchange of genetic information via formation of crossovers (COs). Meiotic recombination
56 results in novel combination of genetic alleles, which enables natural selection can happen in
57 the progenies, and safeguards balanced chromosome segregation that is vital for production of
58 viable gametes and fertility (Wang and Copenhaver, 2018). Meiotic recombination is initiated
59 by generation of DNA double-strand breaks (DSBs) catalyzed by SPO11, that is a type-II
60 topoisomerase (topoisomerase VI, subunit A) conserved among eukaryotes (Bergerat et al.,
61 1997; Grelon et al., 2001; Stacey et al., 2006; Da Ines et al., 2020). Plants with defective DSB
62 formation exhibit impaired homolog synapsis and recombination, and are male sterile due to
63 mis-segregation of chromosomes (Grelon et al., 2001; Stacey et al., 2006; De Muyt et al.,
64 2007; Xue et al., 2018; Da Ines et al., 2020). Subsequently, DSBs are repaired by
65 recombinases RAD51 and DMC1, and eventually are processed into COs or non-COs
66 (Klimyuk and Jones, 1997; Li et al., 2004; Sanchez-Moran et al., 2007; Pohl and Nickoloff,
67 2008; Da Ines et al., 2013; Singh et al., 2017; Su et al., 2017; Kobayashi et al., 2019; Yao et
68 al., 2020). There are two types of COs, most of which belong to type-I class catalyzed by
69 ZMM proteins (i.e., HEI10 and MLH1), and are spaced on chromosomes by interference
70 (Higgins et al., 2004); the other COs (type-II) mediated by MUS81 are interference-
71 insensitive (Hollingsworth and Brill, 2004; Berchowitz et al., 2007).

72

73 DSB formation and meiotic recombination rely on programmed building of chromosome axis
74 and synaptonemal complex (SC). Meiotic-specific cohesion protein AtREC8/SYN1 is a key
75 axis protein, dysfunction of which causes reduced DSB formation and impaired chromosome
76 organization (Zickler and Kleckner, 1999; Lambing et al., 2020b). Two coiled-coil proteins
77 ASY3 and ASY4 participate in organizing axis formation, and mediate the connections
78 between the SYN1-mediated chromosome axis and SC through interplay with HORMA
79 domain protein ASY1, which acts in DMC1-mediated meiotic recombination pathway
80 (Armstrong et al., 2002; Sanchez-Moran et al., 2007; Ferdous et al., 2012; Chambon et al.,
81 2018; Osman et al., 2018). ASY1 prevents preferential occurrence of COs at distal regions by
82 antagonizing telomere-led recombination and maintaining CO interference (Lambing et al.,
83 2020a). The conserved transverse filament protein ZYP1 composes the central element of SC

84 and is crucial for homolog synapsis (Higgins et al., 2005; Wang et al., 2010; Barakate et al.,
85 2014). Recent studies revealed that in Arabidopsis, ZYP1-dependent SC plays a role in
86 shaping type-I CO rate by maintaining CO interference; moreover, the bias of CO rate
87 between sexes is wiped when ZYP1 is knocked out (Capilla-Pérez et al., 2021; France et al.,
88 2021).

89
90 Male meiosis in plants is sensitive to variations of environmental temperature (De Storme and
91 Geelen, 2014; Bomblies et al., 2015; Liu et al., 2019; Lohani et al., 2019). In both dicots and
92 monocots, low temperatures affect cytokinesis by disturbing the formation of phragmoplast,
93 which thereby induces meiotic restitution and formation of unreduced gametes (Tang et al.,
94 2011; De Storme et al., 2012; Liu et al., 2018). Under high temperatures, by comparison, both
95 chromosome dynamics and cytokinesis are impacted; especially, meiotic recombination
96 exhibits complex responses to thermal conditions (Draeger and Moore, 2017; Wang et al.,
97 2017; Mai et al., 2019; De Storme and Geelen, 2020; Lei et al., 2020; Ning et al., 2021;
98 Schindfessel et al., 2021). In Arabidopsis, a mild increase of temperature (28°C) positively
99 affects type-I CO rate by enhancing the activity of ZMM proteins without impacting DSB
100 formation (Lloyd et al., 2018; Modliszewski et al., 2018). At a higher temperature (32°C),
101 however, the rate and distribution of COs are altered and/or reshaped (De Storme and Geelen,
102 2020). When the temperature elevates beyond fertile threshold of Arabidopsis (36-38°C), CO
103 formation is fully suppressed due to inhibited DSB generation and impaired homolog
104 synapsis (Ning et al., 2021). Environmental temperatures therefore may manipulate genomic
105 diversity, and/or influence stability of plant ploidy over generations by impacting male
106 meiosis during microsporogenesis (Bomblies et al., 2015; Lohani et al., 2019).

107
108 Most higher plants, especially for angiosperms, have experienced at least one episode of
109 whole genome duplication (WGD) event, which is considered an important force driving
110 speciation, diversification, and domestication (Dubcovsky and Dvorak, 2007; Leitch and
111 Leitch, 2008; Del Pozo and Ramirez-Parra, 2015; Soltis et al., 2015; Ren et al., 2018).
112 Polyploids are classified into autopolyploids and allopolyploids, which originate from
113 intraspecies WGD events, or arise from multiple evolutionary lineages through the
114 combination of differentiated genomes, respectively (Bretagnolle and Thompson, 1995;
115 Ramsey and Schemske, 1998; Soltis and Soltis, 2009; Jackson and Chen, 2010; Parisod et al.,
116 2010). In autotetraploid plants, four intraspecies-homologues usually undergo randomly
117 separation at anaphase I; this is different as allotetraploids, in which subgenomes tend to
118 segregate independently due to preferential CO formation between the genetically-closer pairs
119 of homologues (Ramsey and Schemske, 2002; Stift et al., 2008). It is considered that the
120 duplicated genome contribute to genomic flexibility and confer plants with enhanced
121 tolerance to both endogenous genetic mutations, or exogenous environmental stresses
122 (Comai, 2005; te Beest et al., 2012; Del Pozo and Ramirez-Parra, 2015; Rao et al., 2020; Van
123 de Peer et al., 2020; Wu et al., 2020). However, the multiple sets of homologous
124 chromosomes also challenge genome stability by impacting chromosome pairing and
125 segregation with associated reduced fertility or viability of plants (Santos et al., 2003; Comai,
126 2005; Otto, 2007; Yant et al., 2013; Svačina et al., 2020). It is proposed that evolutionarily-
127 derived polyploids have developed a moderate strategy that assures genome stability to a

128 large scale by early-stage homoeologous chromosome sorting, modification of chromosome
129 axis-mediated meiotic recombination, and/or by sacrificing CO rate within an acceptable
130 range (Grandont et al., 2014; Bomblies et al., 2016; Lloyd and Bomblies, 2016; Morgan et al.,
131 2020; Seear et al., 2020). But, it remains not yet clear how male meiosis in polyploid plants
132 behaves under thermal stress.

133

134 Here, we comprehensively analyzed meiosis behaviors of colchicine-induced autotetraploid
135 *Arabidopsis* under increased temperatures. We found that a minor proportion of meiosis
136 defects generally takes place in autotetraploid Col-0 under a wide range of temperature
137 conditions, which are significantly increased when temperature reaches extremely high. We
138 showed that heat stress interferes with meiosis in autotetraploid *Arabidopsis* via a prominent
139 impact on chromosome pairing. Cytological analysis revealed that impaired homolog pairing
140 and synapsis, and suppressed CO formation are owing to inhibited DSB generation and SC
141 formation. Moreover, our data supported that heat stress destabilizes lateral structure of SC by
142 targeting chromosome axis, and additionally suggested that stability of chromosome axis and
143 SC in autotetraploid *Arabidopsis* is more sensitive to heat stress than that in diploid
144 *Arabidopsis*. Overall, our findings propose that WGD without natural adaption negatively
145 affects stability and thermal tolerance of meiotic recombination in *Arabidopsis thaliana*,
146 which should be taken into consideration when applying polyploid breeding under the current
147 fast climate-changing background.

148

149

150 **Results**

151

152 **Heat stress increases aberrant meiotic products in autotetraploid *Arabidopsis thaliana***

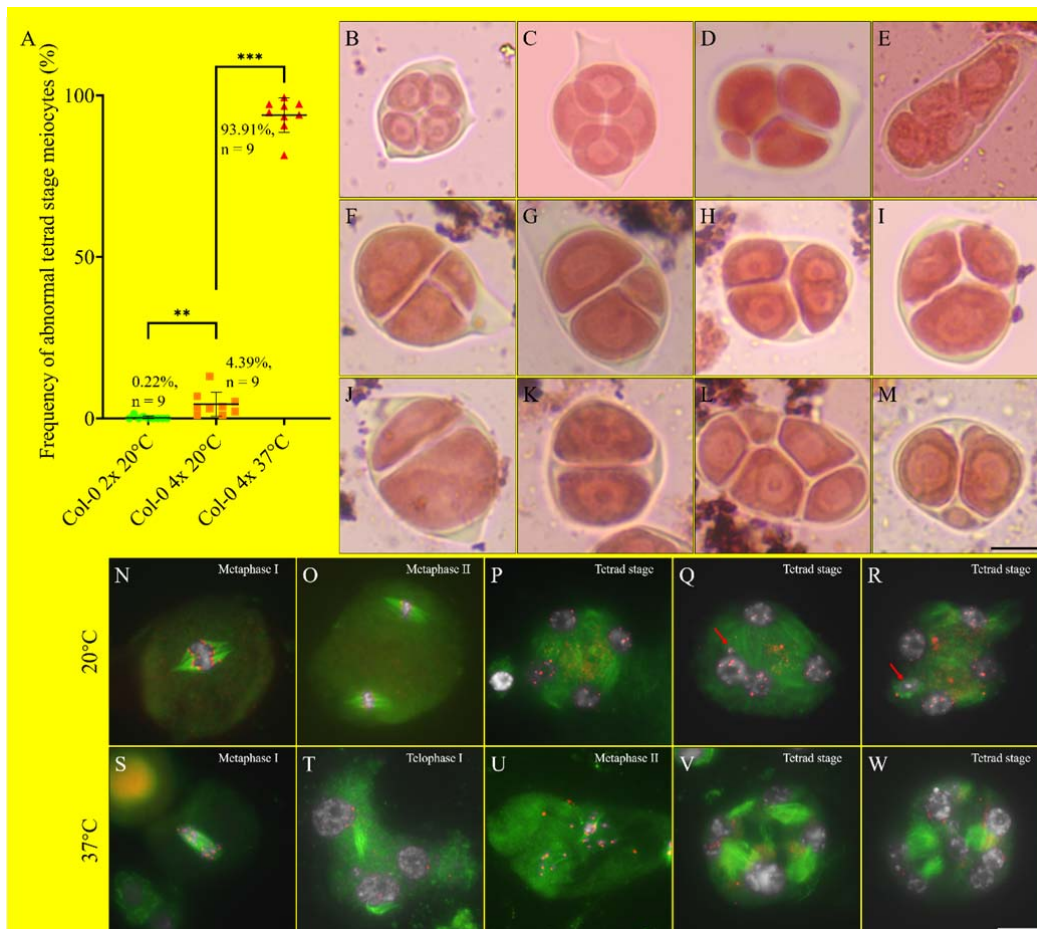
153

154 To address the impact of heat stress on meiosis of autotetraploid *Arabidopsis*, we employed
155 autotetraploid Col-0 plants generated by colchicine treatment on diploid Col-0 as previously
156 reported (De Storme and Geelen, 2011). Fluorescence in situ hybridization (FISH) using a
157 centromere-specific probe in somatic cells confirmed that the plants assayed were tetraploid
158 (Supplemental Fig. S1). Under control temperature (20°C), most PMCs in autotetraploid Col-
159 0 produced tetrads as diploid Col-0 (Fig. 1A-C). Interestingly, every single autotetraploid Col-
160 0 plant was found to yield a small proportion of abnormal meiotic products (Fig. 1A, 4.39%;
161 D and E), which was significantly increased under an extreme high temperature (37°C) (Fig.
162 1A, 93.91%; F-M). Aniline blue staining of tetrad stage meiocytes confirmed occurrence of
163 defective meiotic cytokinesis in autotetraploid Col-0 under both temperature conditions
164 (Supplemental Fig. S2).

165

166 Microtubular cytoskeleton was examined by performing immunolocalization of α -tubulin. At
167 20°C, one and two sets of spindles were built at metaphase I and II, respectively, to separate
168 homologs and sister chromatids (Fig. 1N and O). At telophase II, mini-phragmoplast
169 structures composed of radial microtubule arrays (RMAs) were formed between the four
170 isolated nuclei (Fig. 1P). Notably, as seen by orcein staining, triad- and polyad-like cells were
171 observed, which showed omitted RMA between the two adjacent nuclei (and mini-nucleus,
172 red arrow), or irregular RMA formation between the multiple nuclei (Fig. 1Q and R). After
173 heat treatment, assembly of spindles at metaphase I and II was interfered (Fig. 1S and U);
174 meanwhile, phragmoplast at anaphase I displayed aberrant orientation and sparse microtubule
175 content (Fig. 1T). Most tetrad stage meiocytes exhibited impaired RMA formation (Fig. 1V
176 and W). These findings suggested that male meiosis is unstable in the synthesized
177 autotetraploid *Arabidopsis* grown under normal temperature conditions, which, additionally,
178 is hypersensitive to heat stress.

179



180

181 Figure 1. Analysis of PMCs in autotetraploid Col-0 plants. A, Graph showing the frequency of
 182 abnormal tetrad stage meiocytes in autotetraploid Col-0 plants incubated at 20°C and 37°C. The
 183 numbers indicate the frequency of abnormal tetrad PMCs; n indicates numbers of biological replicates
 184 used for quantification; ** and *** indicate $P < 0.01$ and 0.001 , respectively. B-E, Orcein staining of
 185 tetrad stage meiocytes in diploid Col-0 (B) and autotetraploid Col-0 plants (C-E) grown at 20°C. F-M,
 186 Orcein staining of tetrad stage meiocytes in autotetraploid Col-0 plants stressed by 37°C. N-R,
 187 Immunolocalization of α -tubulin in meiocytes at metaphase I (N), metaphase II (O) and tetrad (P-R)
 188 stages, respectively, of autotetraploid Col-0 plants incubated at 20°C. S-W, Immunolocalization of α -
 189 tubulin in meiocytes at metaphase I (S), anaphase I (T), metaphase II (U) and tetrad (V and W) stages,
 190 respectively, of autotetraploid Col-0 plants stressed by 37°C. Red arrow indicates mini-nucleus. White,
 191 DAPI; green, α -tubulin; red, CENH3. Scale bars = 10 μ m.

192

193 Heat-induced meiosis defects are highly correlated with interfered chromosome pairing

194

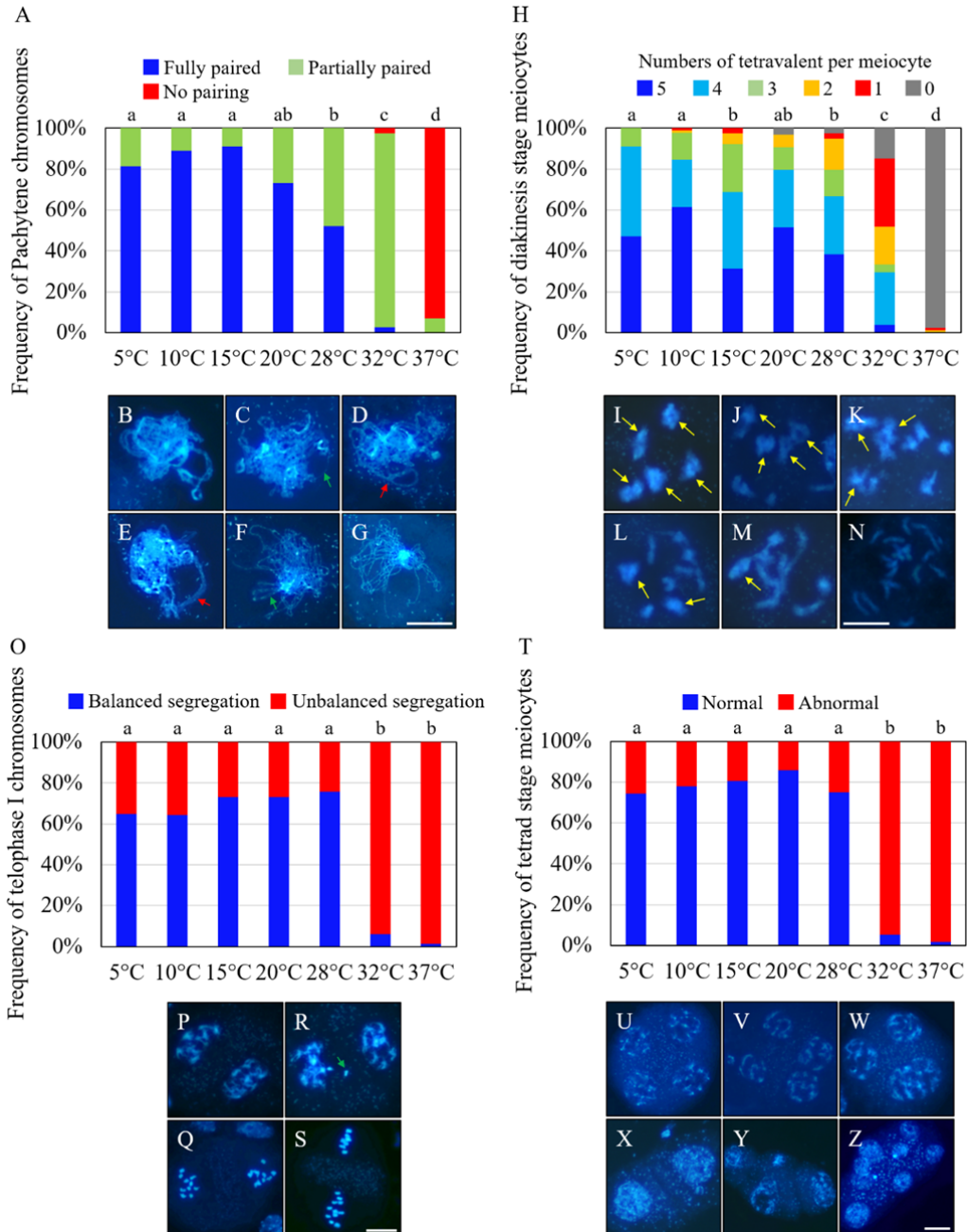
195 Since Arabidopsis plants defective for meiotic recombination (e.g., the *dmc1* mutant) also
 196 show disorganized spindle and phragmoplast during meiosis (Supplemental Fig. S3) (Bai et
 197 al., 1999; Xue et al., 2019; Shi et al., 2021), heat-induced abnormalities in autotetraploid Col-
 198 0 may result from alterations in meiotic recombination. In naturally-derived autotetraploid
 199 Arabidopsis (*A. arenosa*), meiotic recombination rate varies in response to seasonal
 200 temperature changes (Weitz et al., 2021). Driven by the curiosity how meiotic chromosomes

201 in synthesized autotetraploid *Arabidopsis thaliana* would behave under increased
202 temperature, we applied meiotic spreading analysis in autotetraploid Col-0 shocked by a wide
203 range of low-to-high temperatures (i.e., 5, 10, 15, 28, 32 and 37°C, respectively). First,
204 pachytene stage chromosomes were examined to see the impact of temperature elevation on
205 homolog pairing. We found that pairing defect (i.e., homologous chromosomes were not fully
206 paired) existed in autotetraploid Col-0 grown at any given temperature conditions (Fig. 2A-
207 C). Bridge- and/or thick rope-like structures implied an improper chromosome pairing (Fig.
208 2D and E). The frequency of pairing lesions did not show any significant difference at lower
209 temperatures (i.e., 5-20°C) (Fig. 2A). However, as temperature increased, pairing
210 abnormalities were significantly pronounced (Fig. 2A and F), and there was no pairing at
211 37°C (Fig. 2A, $P < 0.01$; G). The rate of successful pairing showed a strong negative
212 correlation with elevated temperatures (Fig. 3A).

213
214 At diakinesis stage, autotetraploid Col-0 plants under low-to-normal temperatures (i.e., 5-
215 20°C) preferentially generate PMCs with five tetravalents, the rate of which was decreased
216 when the temperature climbed to extremely high (Fig. 2H, $P < 0.01$; I-N; Fig. 3B). A positive
217 correlation was found between rate of five-tetravalent formation and successful chromosome
218 pairing (Fig. 3C). Under all the temperatures tested, unbalanced chromosome segregation
219 occurred after meiosis I and II, and showed a significant high level under extreme thermal
220 conditions (Fig. 2O and T, $P < 0.01$; P-S, U-Z). The similar rate of heat-induced irregularities
221 at telophase I and tetrad stage suggested that heat stress induces abnormal meiotic products
222 predominantly by impairing chromosome segregation at meiosis I (Fig. 2O and T; Fig. 3F).
223 Balanced chromosome separation was positively correlated with chromosome pairing status
224 and the ratio of five-tetravalent formation (Fig. 3D and E). Taken together, these data thus
225 suggested that heat stress interferes with chromosome segregation in autotetraploid
226 *Arabidopsis thaliana* via a primary impact on chromosome pairing.

227
228 To address whether meiosis lesions in synthesized autotetraploid *Arabidopsis* generally occurs
229 in polyploid plants, we checked chromosome behaviors in meiocytes of colchicine-induced
230 autotetraploid rice, naturally-derived allotetraploid canola and allohexaploid wheat grown at
231 cultivation temperatures. In both autotetraploid rice and allotetraploid canola, irregular
232 chromosome separation at anaphase I and/or tetrad stage were visualized (Supplemental Fig.
233 S4F; Supplemental Fig. S5A-H); nevertheless, no obvious meiosis defect was observed in
234 allohexaploid wheat (Supplemental Fig. S6A-J). Interestingly, in autotetraploid rice,
235 pachytene stage chromosomes did not show pairing defects (Supplemental Fig. S4A and B),
236 but displayed irregularly arranged chromosomes at metaphase I cell plate (Supplemental Fig.
237 S4C and D, red arrow). These findings hence imply that meiosis instability universally takes
238 place in polyploid plants without evolutionary adaption and/or with genetic instability (Lu et
239 al., 2019).

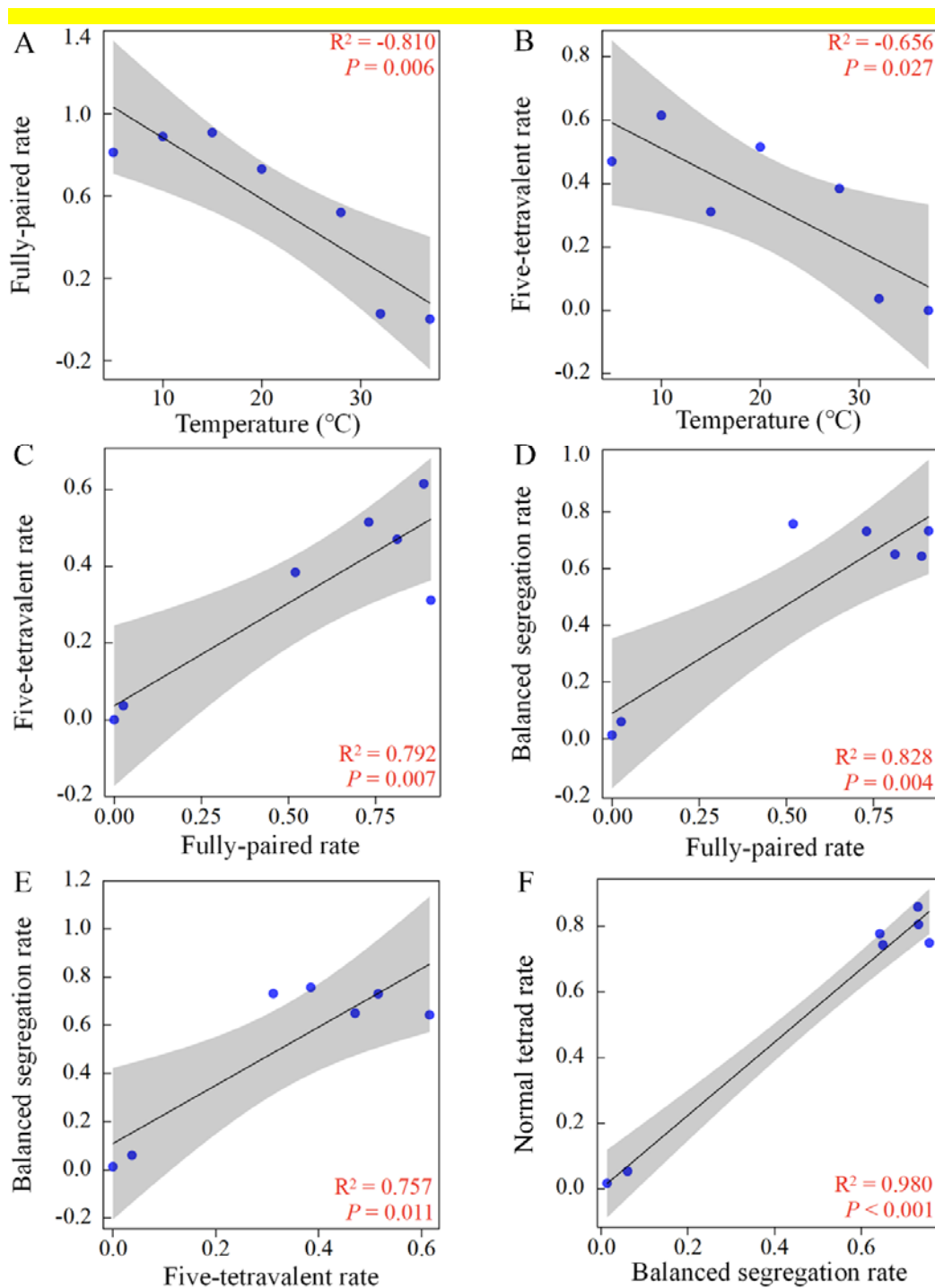
240



241

242 Figure 2. Meiotic chromosome behaviors in autotetraploid Col-0 shocked by different temperatures. A,
 243 Graph showing the frequency of fully-paired, partially-paired and no-pairing pachytene chromosomes
 244 in autotetraploid Col-0 at different temperatures. B-G, Pachytene stage chromosomes showing fully-
 245 paired (B), partially-paired (C), irregularly-associated (D and E), minorly-paired (F) and non-paired
 246 (G) configurations, respectively. Green arrows indicate unpaired chromosomes; red arrows indicate
 247 irregularly-associated chromosomes. H, Graph showing the frequency of diakinesis stage meiocytes
 248 with varied tetraivalent formation in autotetraploid Col-0 at different temperatures. I-N, Diakinesis stage
 249 meiocytes with five (I), four (J), three (K), two (L), one (M) and no (N) tetravalents, respectively.
 250 Yellow arrows indicate tetravalents. O, Graph showing the frequency of telophase I stage meiocytes
 251 showing balanced and/or unbalanced homolog segregation in autotetraploid Col-0 at different

252 temperatures. P-S, Interkinesis (P and R) and metaphase II (Q and S) stage meiocytes showing
253 balanced (P and Q) and unbalanced (R and S) chromosome segregation, respectively. Green arrow
254 indicates lagged chromosome. T, Graph showing the frequency of normal and/or abnormal tetrad stage
255 meiocytes in autotetraploid Col-0 at different temperatures. U-Z, Tetrad stage meiocytes showing
256 normal (U) and abnormal (V-Z) configurations. Nonparametric and unpaired *t* test was performed.
257 Lower letters indicate significant difference between different temperatures by setting significance
258 level $P < 0.05$. Original quantification data and number of cells quantified were supplied in Supplement
259 Table S1-S4. Scale bars = 10 μm .
260



261

262 **Figure 3. Correlation between chromosome behaviors of autotetraploid Col-0 at different temperature**
263 **conditions. A and B, Correlations between frequency of chromosome pairing (A) and five-tetavalent**
264 **formation (B) with temperature variations. C and D, Correlations between frequency of five-tetavalent**
265 **formation (C) and balanced chromosome segregation at anaphase I (D) with rate of fully-pairing of**
266 **pachytene chromosomes. E, Correlation between frequency of balanced chromosome segregation at**
267 **anaphase I with rate of five-tetavalent formation. F, Correlation between frequency of normal tetrad**
268 **formation with rate of balanced chromosome segregation at anaphase I.**

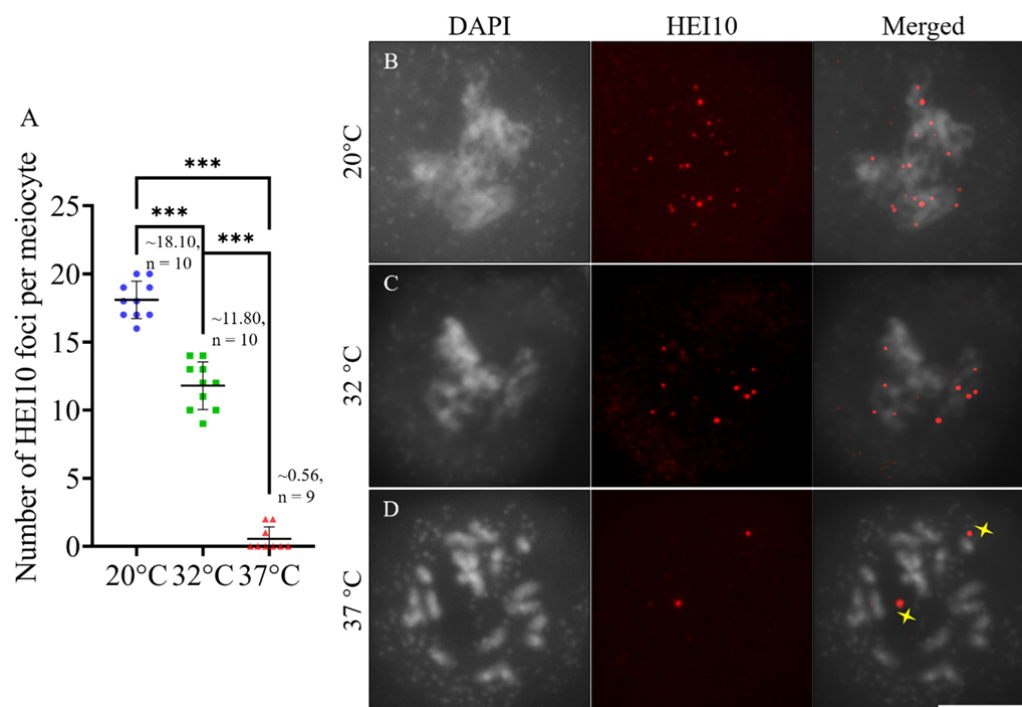
269

270 Type-I CO rate is lowered in autotetraploid Arabidopsis under high temperatures

271

272 Univalent formation in autotetraploid Col-0 plants under high temperatures suggested that CO
273 formation was compromised or suppressed. To this end, we performed immunolocalization of
274 HEI10 protein, which marks class I-type CO (Chelysheva et al., 2012; Wang et al., 2012), and
275 quantified its abundance on the diakinesis chromosomes. At 20°C, autotetraploid Col-0
276 showed an average of 18.10 HEI10 foci per meiocyte (Fig. 4A and B), which was reduced to
277 an average of 11.80 and 0.56 in the plants stressed by 32°C and 37°C, respectively (Fig. 4C
278 and D). This data indicated that high temperatures inhibit formation of class I-type CO in
279 autotetraploid Arabidopsis.

280



281

282 Figure 4. Immunolocalization of HEI10 on diakinesis chromosomes in autotetraploid Col-0 plants
283 under increased temperatures. A, Graph showing the number of HEI10 foci per diakinesis-staged
284 meiocyte. Numbers indicate the average number of HEI10 foci per meiocyte; n indicates the number of
285 cells quantified; *** indicates $P < 0.001$. B-D, Immunolocalization of HEI10 on diakinesis
286 chromosomes of autotetraploid Col-0 plants incubated at 20°C (B), 32°C (C) and 37°C (D). Yellow
287 stars indicate non-specific foci to HEI10. Scale bar = 10 μm .

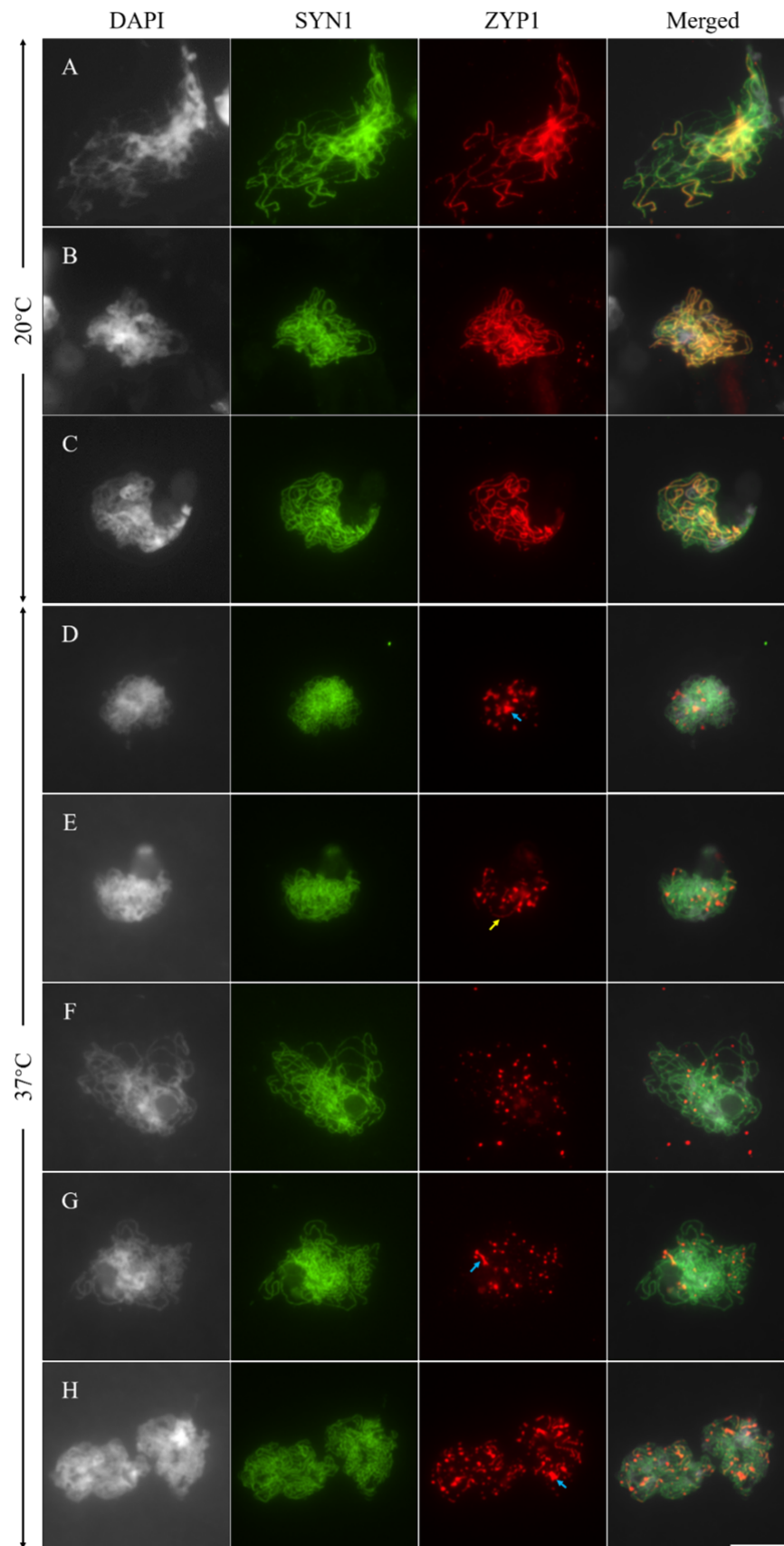
288

289 Heat stress impairs SC assembly in autotetraploid Arabidopsis

290

291 SC assembly is required for homolog synapsis (Higgins et al., 2005; Wang et al., 2010;
292 Barakate et al., 2014; Capilla-Pérez et al., 2021; France et al., 2021), we subsequently
293 examined central element of SC in heat-stressed autotetraploid Col-0 plants by performing
294 immunolocalization of ZYP1 protein, the core element of transverse filament. At 20°C,

295 zygotene meiocytes displayed partially-assembled linear ZYP1 configuration (Fig. 5A).
296 Thereafter ZYP1 were fully assembled at the central region of the paired homologs at middle
297 pachytene, and were gradually disassociated as disintegration of SC from late pachytene (Fig.
298 5B and C). By contrast, plants stressed by 37°C displayed dotted and/or fragmented
299 installation of ZYP1 from early zygotene to late pachytene (Fig. 5D-H, yellow arrow), which
300 indicated that assembly of SC was impaired. Aggregated and/or enlarged ZYP1 foci hinted
301 pairing between multiple chromosomes (Fig. 5D, G and H, blue arrows) (Loidl, 1989;
302 Morgan et al., 2017; Ning et al., 2021). Localization of SYN1 did not show any obvious
303 defect indicating that heat stress does not affect SYN1-mediated axis (Fig. 5D-H). Moreover,
304 in line with the chromosome spreading analysis, ZYP1 loading was not influenced by cold
305 (5°C) (Supplemental Fig. S7A-C), but was slightly impacted under mildly increased
306 temperature (28°C) (i.e., incomplete ZYP1 loading occurring at unpaired chromosome
307 regions (Supplemental Fig. S7D-F, red arrow).
308



309

310 Figure 5. Co-immunolocalization of SYN1 and ZYP1 in meiocytes of autotetraploid Col-0 plants. A-C,
311 Zygotene- (A), middle pachytene- (B) and late pachytene-staged (C) meiocytes in autotetraploid Col-0
312 at 20°C. D-H, Early zygotene- (D), middle zygotene- (E), late zygotene- (F), middle pachytene- (G)
313 and late pachytene-staged (H) meiocytes in autotetraploid Col-0 stressed by 37°C. Green, SYN1; red,
314 ZYP1. Yellow arrow indicates fragmented ZYP1 signals. Blue arrows indicate aggregated and/or
315 enlarged ZYP1 foci. Scale bar = 10 μ m.

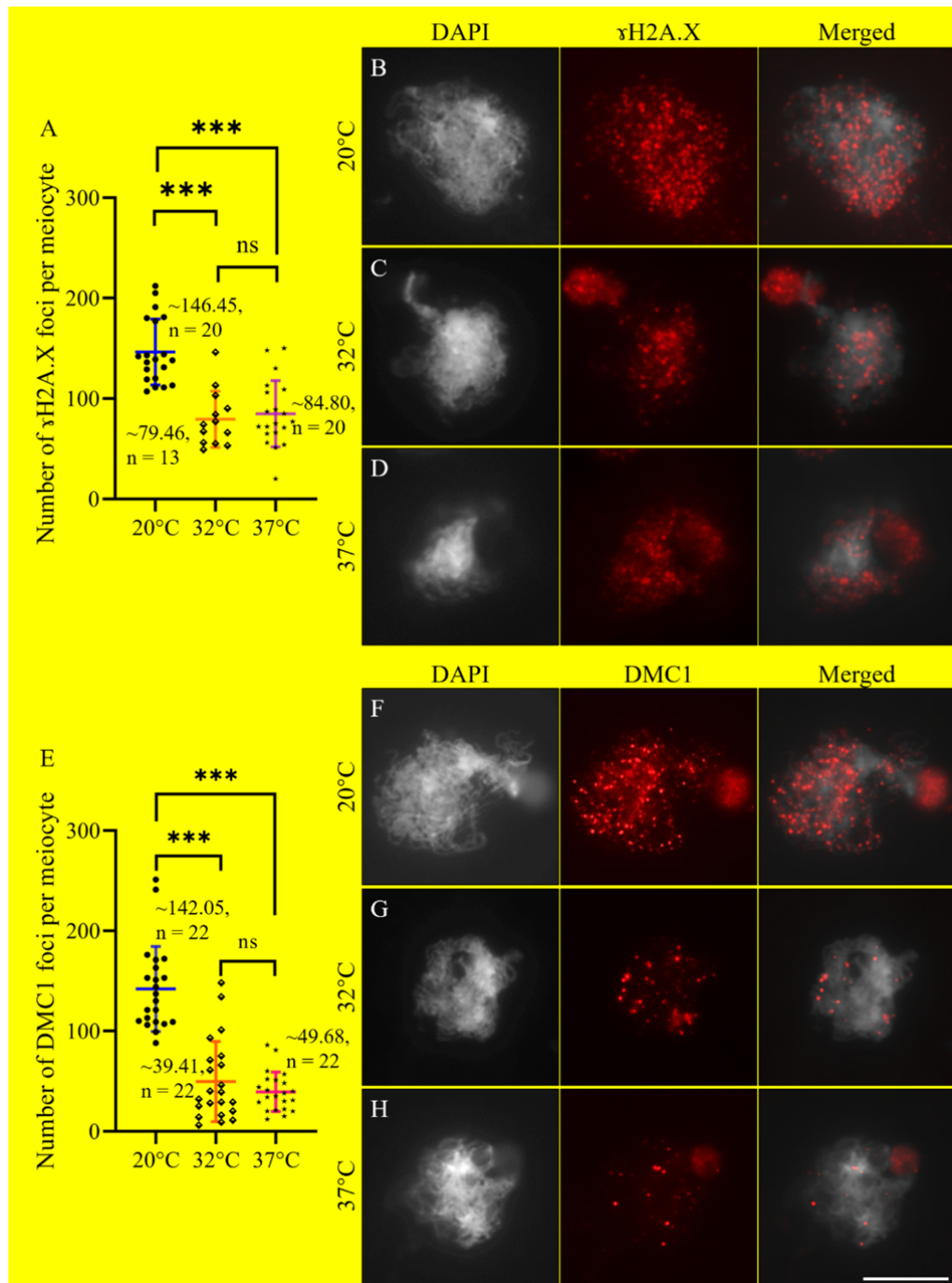
316

317 **Heat stress reduces DSB formation in autotetraploid Arabidopsis**

318

319 DSB generation is crucial for homolog pairing and CO formation (De Muyt et al., 2007;
320 Hartung et al., 2007; Kurzbauer et al., 2012). To address whether heat-interfered chromosome
321 pairing and CO reduction was owing to compromised DSB formation, we indirectly scored
322 DSB abundance by counting the number of γ H2A.X, which specifically marks
323 phosphorylated histone variant H2A.X at DSB sites (Kurzbauer et al., 2012). Autotetraploid
324 Col-0 incubated at 20°C showed an average of 146.5 γ H2A.X foci per meiocyte at zygotene,
325 and was lowered to 79.46 and 84.8 per meiocyte when the temperature was elevated to 32°C
326 and 37°C, respectively (Fig. 6A-D). In addition, the number of DMC1 on zygotene
327 chromosomes decreased under the high temperatures, either (Fig. 6E-H). These data indicated
328 that DSB formation is compromised in heat-stressed autotetraploid Arabidopsis.

329



330
 331 Figure 6. Immunolocalization of γ H2A.X and DMC1 on zygote chromosomes of autotetraploid Col-
 332 0 plants. A, Graph showing the number of γ H2A.X foci per meiocyte in autotetraploid Col-0 plants at
 333 20°C, 32°C and 37°C. B-D, Immunolocalization of γ H2A.X on zygote chromosomes of
 334 autotetraploid Col-0 plants grown at 20°C (B), 32°C (C) and 37°C (D), respectively. E, Graph showing
 335 the number of DMC1 foci per meiocyte in autotetraploid Col-0 plants at 20°C, 32°C and 37°C. F-H,
 336 Immunolocalization of DMC1 on zygote chromosomes of autotetraploid Col-0 plants at 20°C (F),
 337 32°C (G) and 37°C (H), respectively. Numbers indicate the average number of γ H2A.X or DMC1 foci
 338 per meiocyte; n indicates the number of cells quantified; *** indicates $P < 0.001$; ns indicates no
 339 significant difference. Scale bars = 10 μ m.

340

341

Higher heat-sensitivity of chromosome axis in autotetraploid Arabidopsis

342

343

Successful homolog synapsis and CO formation also rely on normal assembly of chromosome

344

axis. Since SYN1 is not impacted by heat stress, we examined the dynamics of two other

345

axis-associated proteins (i.e., ASY1 and ASY4) in autotetraploid Col-0. In control plants,

346

linear SYN1 and ASY1 overlapped and were associated with the entire chromosomes at

347

zygotene (Fig. 7A and B). ASY1 were unloaded at some chromosome regions at pachytene

348

when homolog fully synapsed (Fig. 7C and D). After heat treatment, most zygotene and

349

pachytene chromosomes in autotetraploid Col-0 displayed dotted configuration of ASY1,

350

whose frequency was significantly higher than that in heat-stressed diploid Col-0 (Fig. 7E-H;

351

Supplemental Fig. S8; Supplemental Fig. S10A-C). Similar phenotypic alterations have been

352

observed in ASY4 loading in heat-stressed autotetraploid Col-0 (Fig. 8A-E; Supplemental

353

Fig. S9; Supplemental Fig. S10D-F). These hinted that ASY1- and ASY4-mediated

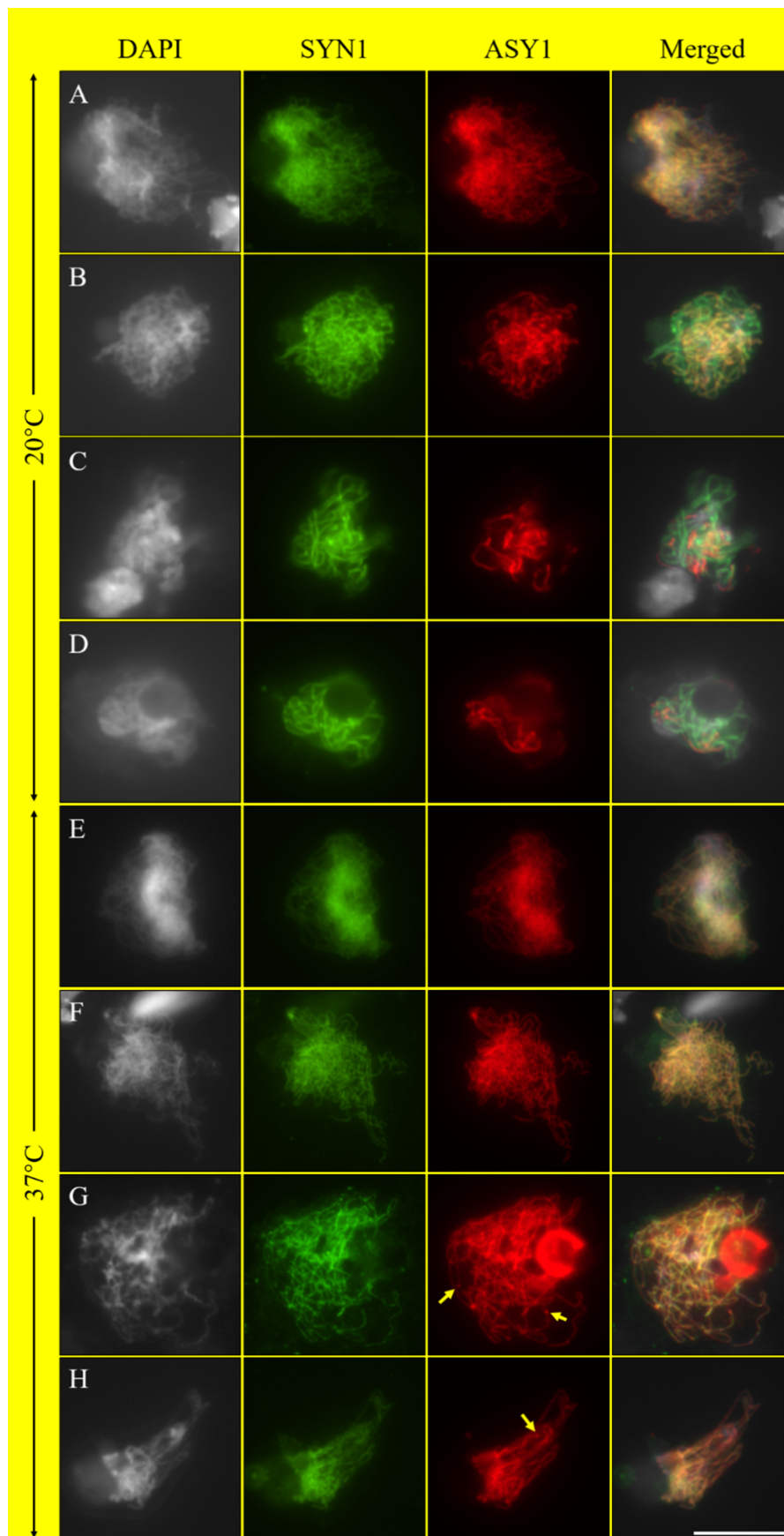
354

chromosome axis in autotetraploid Arabidopsis is more sensitive to heat than that in diploid

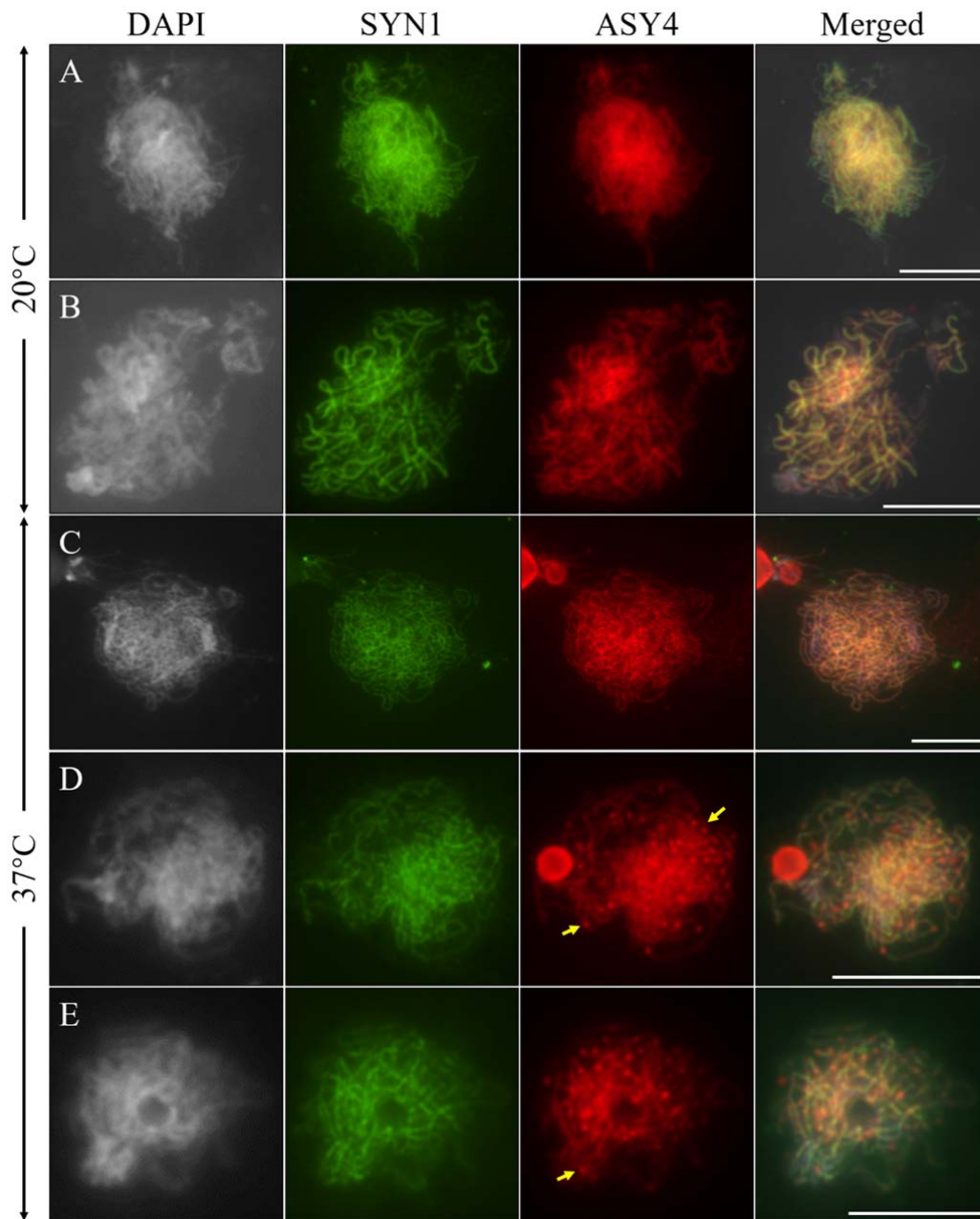
355

Arabidopsis.

356



358 Figure 7. Co-immunolocalization of SYN1 and ASY1 in meiocytes of autotetraploid Col-0 plants. A-D,
359 Early zygotene (A), middle zygotene (B), middle pachytene (C) and late pachytene (D) chromosomes
360 in autotetraploid Col-0 plants at 20°C. E-H, Zygotene (E and G) and pachytene (F and H)
361 chromosomes showing linear (E and F) and dotted (G and H) configurations, respectively, in
362 autotetraploid Col-0 plants at 37°C. Green, SYN1; red, ASY1. Yellow arrows indicate dotted ASY1
363 foci. Scale bar = 10 µm.
364



365
366 Figure 8. Co-immunolocalization of SYN1 and ASY4 in meiocytes of autotetraploid Col-0 plants. A
367 and B, Zygotene (A) and pachytene (B) chromosomes in autotetraploid Col-0 plants at 20°C. C-E,
368 Zygotene (C and D) and pachytene (E) chromosomes showing linear (C) and dotted (D and E)

369 configurations, respectively, in autotetraploid Col-0 plants at 37°C. Green, SYN1; red, ASY4. Yellow
370 arrows indicate dotted ASY4 foci. Scale bars = 10 µm.

371

372 **Heat stress affects lateral element of SC by impacting stability of chromosome axis**

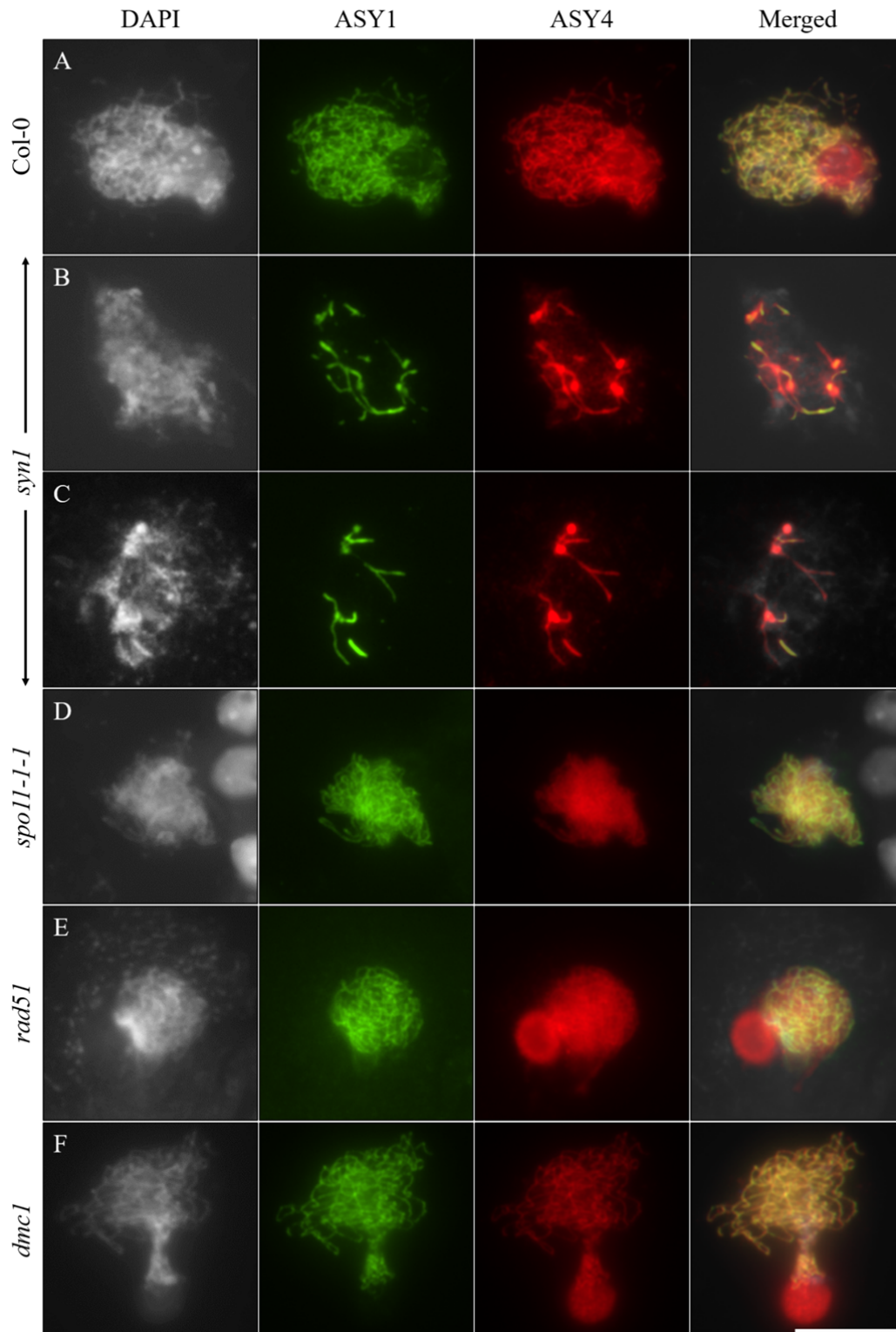
373

374 It is proposed that assembly of ASY1-associated lateral element of SC relies on a step-wise
375 formation of SYN1-ASY3-ASY4-mediated chromosome axis (Ferdous et al., 2012; Chambon
376 et al., 2018; Lambing et al., 2020b). We performed co-immunolocalization of ASY1 and
377 ASY4 in diploid Col-0, and the *syn1*, *spo11-1-1*, *rad51* and *dmc1* mutants (Fig. 9). In the
378 wild-type and the *spo11-1-1*, *rad51* and *dmc1* mutants, ASY1 and ASY4 co-localize on
379 middle zygotene chromosomes (Fig. 9A; D-F). By contrast, the *syn1* mutant displayed
380 incomplete and/or fragmented ASY1 and ASY4 loading, which additionally overlapped on
381 the zygotene and pachytene chromosomes (Fig. 9B and C). These observations are in line
382 with the opinion that DSB processing is downstream of axis assembly, and ASY1-associated
383 SC formation relies on ASY4-mediated axis formation, which in turn depends on functional
384 SYN1.

385

386 Considering the similarities of defective ASY1 and ASY4 loading under heat stress, and the
387 upstream action of axis formation on SC assembly, we hypothesized that heat stress
388 destabilizes ASY1-associated lateral regions of SC via an impacted ASY4 stability. To this
389 end, a combined immunostaining of ASY1 and ASY4 was applied in the heat-stressed diploid
390 and autotetraploid Col-0 plants. Under control temperature, ASY1 and ASY4 co-localized on
391 the early and middle zygotene chromosomes of diploid and autotetraploid Col-0 (Fig. 10A,
392 diploid Col-0; D, autotetraploid Col-0; Supplemental Fig. S11A and B, autotetraploid Col-0).
393 Subsequently, ASY1 started to be unloaded off the chromosomes from early pachytene, while
394 ASY4 kept a complete linear configuration (Supplemental Fig. S11C-E), indicating that
395 ASY4 is disassembled later than ASY1 (Supplemental Fig. S11F and G). Notably, in both the
396 diploid and autotetraploid Col-0, heat-induced incomplete and/or dotted ASY1 and ASY4
397 signals co-localized on the chromosomes (Fig. 10B and C, diploid Col-0; E and F,
398 autotetraploid Col-0; yellow arrows). It thus is likely that heat stress affects ASY1-associated
399 SC via compromised stability of ASY4-mediated chromosome axis.

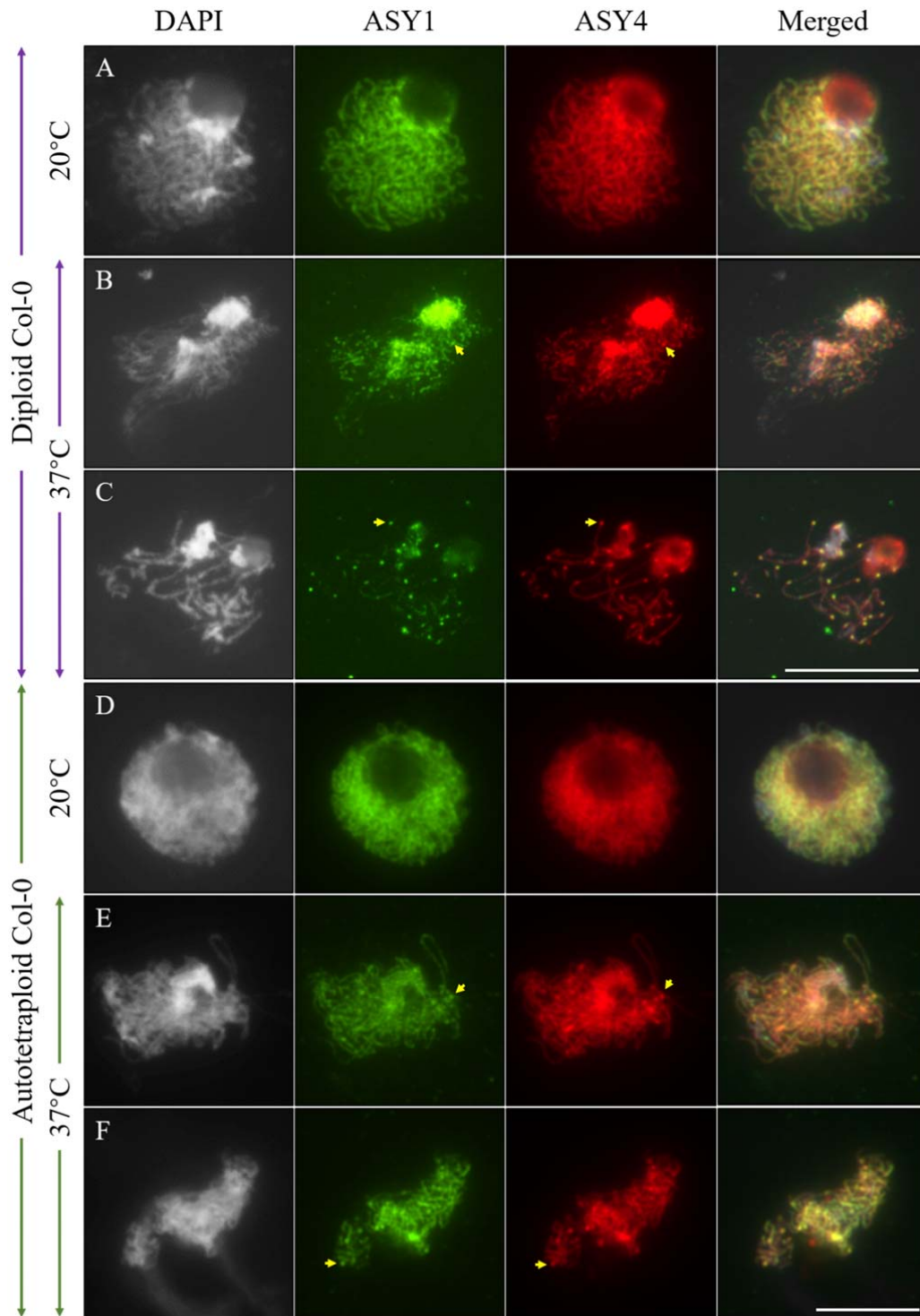
400



401

402 Figure 9. Co-immunolocalization of ASY1 and ASY4 in meiocytes of diploid wild-type Col-0, and the
403 *syn1*, *spo11-1-1*, *rad51* and *dmc1* mutants. A-F, Zygotene chromosomes in diploid Col-0 (A); zygotene
404 (B) and pachytene (C) chromosomes in the *syn1* mutant; zygotene chromosomes in the *spo11-1-1* (D),
405 *rad51* (E) and the *dmc1* (F) mutants. Green, ASY1; red, ASY4. Scale bar = 10 μ m.

406



407

408

409

410

411

412

Figure 10. Co-immunolocalization of ASY1 and ASY4 in heat-stressed diploid and autotetraploid Col-0 plants. A and D, Zygotene-staged meiocytes in diploid (A) and autotetraploid (D) Col-0 plants grown at 20°C. B and C, Zygotene- (B) and pachytene-staged (C) meiocytes in heat-stressed diploid Col-0. E and F, Zygotene- (E) and pachytene-staged (F) meiocytes in autotetraploid Col-0 at 37°C. Green, ASY1; red, ASY4. Yellow arrows indicate co-localization of dotted ASY1 and ASY4 foci. Scale bars =

413 10 μm .

414

415

416 Discussion

417

418 **Meiosis is unstable in autotetraploid *Arabidopsis thaliana* without natural adaption**

419

420 WGD is a conserved phenomenon that contributes to genomic diversity and speciation in
421 higher plants (Comai, 2005; Dubcovsky and Dvorak, 2007; te Beest et al., 2012; Ren et al.,
422 2018; Van de Peer et al., 2020; Li et al., 2021). Additional copies of chromosomes, however,
423 also increase the complexity and challenge for homolog pairing and synapse which eventually
424 harms balanced chromosome segregation at later meiosis stages (Yant et al., 2013; Lloyd and
425 Bomblies, 2016; Svačina et al., 2020; Li et al., 2021). In this study, we found that synthesized
426 autotetraploid Col-0 yields a low but consistently-detectable rate of aberrant meiotic products
427 under normal temperature conditions (Fig. 1). Chromosome analysis revealed that
428 unsuccessful pairing and unbalanced chromosome segregation occur in autotetraploid
429 *Arabidopsis* grown under a wide range of low-to-high temperatures (Fig. 2). The co-aligned,
430 but un-synapsed axis regions suggest that the synapsis defects are (or at least in part)
431 independent of defects in chromosome pairing (Fig. 2F) (Capilla-Pérez et al., 2021; France et
432 al., 2021). The autotetraploid Col-0 plants that we used here is very typical of neo-
433 autotetraploids that are considered genetically unstable compared with the evolution-derived
434 autotetraploids (e.g., *A. lyrata* and *A. arenosa*) (Yant et al., 2013; Henry et al., 2014; Lloyd
435 and Bomblies, 2016). In support, synthesized autotetraploid rice and naturally-derived
436 allotetraploid canola, which, however, is genetically unstable (Lu et al., 2019), also show
437 defective segregation of homologous chromosomes (Supplemental Fig. S4F; Supplemental
438 Fig. S5B-D). By contrast, meiosis in evolutionarily-derived hexaploid *Triticum aestivum*
439 behaves normally (Supplemental Fig. S6) (El Baidouri et al., 2017). The meiotic defects we
440 observed here hence are probably the effect of polyploidization without natural adaption
441 and/or evolutionary selection. On the other hand, in synthesized autotetraploid rice, we did
442 not find pachytene chromosomes with pairing defects (Supplemental Fig. S4A and B),
443 suggesting that meiosis alterations in autotetraploid rice may not be caused by interfered
444 homolog pairing but by other disorders; e.g., improper multivalent dissolution (Supplemental
445 Fig. S4D) (Lloyd and Bomblies, 2016). Therefore, the mechanisms of WGD interfering with
446 meiosis may vary among species.

447

448 **Increased temperatures impose a dominant impact on chromosome pairing**

449

450 We found that the rate of successful chromosome pairing and tetravalent formation were not
451 altered under 5-20°C, suggesting that homolog pairing and CO formation are more sensitive
452 to high temperatures (Fig. 2A and H; Supplemental Fig. S7A-C). Autotetraploid *Arabidopsis*
453 primarily generates diakinesis PMCs that contain five tetravalents (Fig. 2H), which is in line
454 with the notion that autotetraploids preferentially undergo synapsis between four homologous
455 chromosomes when environmental temperature is suitable for meiotic recombination (Lloyd
456 and Bomblies, 2016; Svačina et al., 2020; Braz et al., 2021). The negative correlation between
457 chromosome pairing, tetravalent formation and increased temperatures imply that high
458 temperatures affect CO formation predominantly by interfering with homolog pairing (Fig.

459 3A-C). Similarly, in naturally-derived autotetraploid *Arabidopsis*, multivalent formation is
460 strongly correlated with seasonal temperature alterations (Weitz et al., 2021). Polyploid plants
461 thus may apply same (at least very similar) mechanism in response to climate changes during
462 meiotic recombination.

463
464 Heat-induced DSB reduction could be one of the main causes of impaired chromosome
465 pairing in heat-stressed *Arabidopsis* (Fig. 6), which, additionally, may be a conserved
466 phenomenon among eukaryotes (Pohl and Nickoloff, 2008; Ning et al., 2021). But this effect
467 is not likely to be caused by a direct impact on the expression of DSB formation factors (i.e.,
468 *SPO11-1*, *PRD1*, 2 and 3) (Ning et al., 2021). Notably, the expression of phosphatidylinositol
469 3 kinase-like (PI3K) protein kinase *Ataxia-Telangiectasia Mutated (ATM)*, which undertakes a
470 conserved function in sensing DNA damage and evoking DSB repair events (reviewed by
471 (Paull, 2015)), is elevated under heat stress (Ning et al., 2021). In multiple species, the
472 activity of ATM is negatively correlated with DSB abundance (Joyce et al., 2011; Lange et al.,
473 2011; Zhang et al., 2011; Carballo et al., 2013; Garcia et al., 2015; Mohibullah and Keeney,
474 2017; Shi et al., 2019). In *Arabidopsis*, ATM limits DSB formation by restricting the
475 accumulation of SPO11 on prophase I chromosomes (Yao et al., 2020; Kurzbauer et al.,
476 2021). Therefore, it is possible that high temperatures interfere with DSB formation via an
477 over-activated ATM function. On the other hand, our data suggest that high temperatures can
478 directly disorder SC formation, since autotetraploid *Arabidopsis* stressed by 32°C has similar
479 level of DSB as at 37°C, but exhibits a mildly-compromised rate of successful chromosome
480 pairing and CO formation (Fig. 2, 4 and 6) (De Storme and Geelen, 2020).

481
482 **Heat stress affects lateral element of SC by impacting ASY4-mediated chromosome axis**

483
484 The loading of ASY1 and ASY4 is compromised in the *syn1* mutant (Fig. 9B and C) (Ning et
485 al., 2021), which, however, is not the case conversely (Ferdous et al., 2012; Chambon et al.,
486 2018; Lambing et al., 2020b). Meanwhile, linear configuration of ASY3 depends on
487 functional ASY4 (Chambon et al., 2018). Therefore, SYN1, ASY4 and ASY3 may act by a
488 stepwise manner in mediating axis formation. However, since ASY4 directly interacts with
489 ASY3, the normal loading of ASY4 thus may also rely on the existence of ASY3 (Chambon
490 et al., 2018). The slower unloading of ASY4 than ASY1 on later prophase I chromosomes
491 supports that SC assembly is downstream of axis formation (Supplemental Fig. S9)
492 (Chelysheva et al., 2005; Ferdous et al., 2012; Chambon et al., 2018; Lambing et al., 2020a;
493 Lambing et al., 2020b). Heat-induced ASY1 and ASY4 abnormalities occur at a similar
494 frequency, which, meanwhile, co-localize on the chromosomes (Fig. 10; Supplemental Fig.
495 S10). These data hence support the hypothesis that high temperatures destabilize lateral
496 structure of SC via impacted chromosome axis. Since SYN1 keeps stable under the high
497 temperatures (Fig. 5, 7 and 8) (Ning et al., 2021), it is plausible that heat stress specifically
498 targets the ‘bridge’ function of ASY4 and/or ASY3 that associate chromosome axis with SC.
499 Whether the impacted axis stability also channels the compromised DSB formation under
500 heat stress remain further investigation.

501
502 **WGD does not increase thermal tolerance of meiosis in *Arabidopsis thaliana***

503

504 Polyploid plants are considered to have evolutionarily developed enhanced tolerance to
505 genetic variations due to higher gene copies, and to abiotic stresses via modulated hormone
506 metabolism and/or reprofiled gene expression (Allario et al., 2013; Lourkisti et al., 2020; Rao
507 et al., 2020; Van de Peer et al., 2020). However, the significantly reduced abundance of
508 γ H2A.X and DMC1 in autotetraploid Col-0 plants under high temperatures suggest that the
509 duplicated genome does not change the thermal threshold of DSB formation in *Arabidopsis*
510 *thaliana* (Fig. 6) (Ning et al., 2021). The slightly increased defect of chromosome pairing at
511 28°C (Fig. 2A; Supplemental Fig. S7), which does not occur in diploid *Arabidopsis*
512 (Modliszewski et al., 2018), implies that homolog pairing and/or synapsis in autotetraploid
513 *Arabidopsis* is also more heat-sensitive. Meanwhile, autotetraploid *Arabidopsis* shows higher
514 rate of impacted ASY1- and ASY4-mediated chromosome axis to heat shock (Supplemental
515 Fig. S10). Our findings thus suggest that genome duplication does not promote thermal
516 tolerance of meiotic recombination in *Arabidopsis thaliana*. Indeed, chromosome axis
517 components plays an important role in maintaining meiosis stability in tetraploid *Arabidopsis*,
518 whose expression is high temperature-sensitive (Morgan et al., 2020; Ning et al., 2021).
519 Therefore, polyploidization-induced higher stress tolerance may not be a general event. One
520 of the explanation could be that environmental stimulus modulates gene expression in a
521 tissue-specific manner in polyploids (Adams and Wendel, 2005). Alternatively, enhanced axis
522 instability under heat shock may be attributed to an increased complexity of chromosome
523 organization in autotetraploid *Arabidopsis* plants which has not experienced evolutionary
524 adaption (Morgan et al., 2020; Seear et al., 2020; Svačina et al., 2020).

525

526 **Materials and methods**

527

528 **Plant materials and growth conditions**

529

530 Diploid and autotetraploid *Arabidopsis thaliana* Columbia-0 (Col-0), autotetraploid rice (*O.*
531 *sativa* L. ssp. *Indica* cv. 9311) (Gan et al., 2021), hexaploid *Triticum aestivum* cultivar ‘Fielder’,
532 allotetraploid canola (*Brassica napus* cv. Westar), the *atsyn1-1* (SALK_137095), *atrad51*
533 (SAIL_873_C08), *atspo11-1-1* (Grelon et al., 2001) and the *atdmc1* (SALK_056177) mutants
534 were used in the study. The autotetraploid Col-0 plants were generated by colchicine
535 treatment on diploid Col-0 plants as described previously (De Storme and Geelen, 2011), and
536 have been propagated around five generations. Determination of chromosome number was
537 performed in somatic cells by fluorescence in situ hybridization. *Arabidopsis* plants were
538 grown under a 16 h day/8 h night, 20°C, and 50% humidity condition. Rice plants were
539 grown in paddy fields during the growing season in Wuhan (30.52°N, 114.31°E), China.
540 Canola and wheat were grown in a growth chamber with a 16 h day/8 h night and 22°C
541 condition.

542

543 **Temperature treatment**

544

545 Young flowering plants were transferred from control temperature (20°C) to a humid chamber

546 with a 16 h day/8 h night and incubated at 5°C, 10°C, 15°C, 28°C, 32°C and 37°C,
547 respectively, and were treated for 24 h. All the treatment started from 8:00-10:00 AM.
548 Meiosis-staged flower buds were fixed by carnoy's fixative or paraformaldehyde upon the
549 finish of treatment.

550

551 **Cytology and fluorescence in situ hybridization**

552

553 Meiotic chromosome behaviors were analyzed by performing chromosome spreading using
554 meiosis-staged flower buds fixed at least 24 h by carnoy's fixative. Flower buds were washed
555 twice by distilled water and once in citrate buffer (10 mM, pH = 4.5), and were incubated in
556 digestion enzyme mixture (0.3% pectolyase, 0.3% cellulase and 0.3% cytohelicase) in citrate
557 buffer (10 mM, pH = 4.5) at 37°C in a moisture chamber for 2.5-3.5 h. Subsequently, 6-8
558 digested buds were washed in distilled water, and were transferred to a glass slide followed by
559 squashing with a small amount (4-5 µL) of distilled water. Two rounds of 10 µL precooled
560 60% acetic acid were added to the samples and were stirred gently, after which the slide was
561 transferred to a hotplate at 45°C for 1-2 min, and thereafter was flooded with precooled
562 carnoy's fixative. The slides were subsequently air dried for 10 min, and were stained by
563 adding 8 µL DAPI (10 µg/mL) in Vectashield antifade mounting medium, mounted with a
564 coverslip, and sealed by nail polish. To analyze and quantify meiotic products, tetrad-staged
565 flower buds were stained by 45% orcein, and the flower buds containing significant number
566 of tetrad-staged PMCs were used for quantification. Five biological replicates were analyzed
567 both for control and heat-stressed plants. To analyze meiotic cytokinesis, tetrad-staged flower
568 buds were stained by aniline blue (0.1% in 0.033% K₃PO₄). FISH assay and the centromere-
569 specific probe have previously been reported (Lei et al., 2020). For rice, canola and wheat,
570 young panicles were fixed with carnoy's fixative, and anthers containing PMCs occurring
571 meiosis were squashed followed by 45% orcein staining or chromosome spreading analysis.

572

573 **Generation of antibodies**

574

575 The anti-AtSYN1 antibodies were raised in rabbits and mouse, respectively, as previously
576 reported (Bai et al., 1999); the anti-AtASY1 antibodies were generated in rabbits and mouse,
577 respectively, against amino acid sequence SKAGNTPISNKAQPAASRES of AtASY1
578 conjugated to KLH; the anti-AtZYP1 antibody (rat) was generated against the amino acid
579 sequence GSKRSEHIRVRSNDNDNVQD of AtZYP1A conjugated to KLH.

580

581 **Immunolocalization of MR proteins and α -tubulin**

582

583 Immunostaining of α -tubulin and MR proteins was performed as reported (Chelysheva et al.,
584 2010; Wang et al., 2014; Liu et al., 2017). Antibodies against ZYP1 (rabbit and/or rat) (Ning
585 et al., 2021), HEI10 (rabbit), DMC1 (rabbit) (Ning et al., 2021) and γ H2A.X (rabbit)
586 (Lambing et al., 2020b) were diluted by 1:100; antibodies against α -tubulin (rat) (Lei et al.,
587 2020), ASY1 (rabbit and/or mouse), ASY4 (rabbit) (Ning et al., 2021) and SYN1 (mouse)
588 were diluted by 1:200; antibody against CENH3 (rabbit) (Abcam, 72001) was diluted by
589 1:400; antibody against SYN1 (rabbit) was diluted by 1:500. The secondary antibodies; i.e.

590 Goat anti-Rabbit IgG (H+L) Cross-Adsorbed Secondary Antibody Alexa Fluor 555
591 (Invitrogen, A32732), Goat anti-Rabbit IgG (H+L) Highly Cross-Adsorbed Secondary
592 Antibody Alexa Fluor Plus 488 (Invitrogen, A32731), Goat anti-Rat IgG (H+L) Cross-
593 Adsorbed Secondary Antibody, Alexa Fluor 555 (Invitrogen, A21434), Goat anti-Rat IgG
594 (H+L) Cross-Adsorbed Secondary Antibody, Alexa Fluor 488 (Invitrogen, A11006) and Goat
595 anti-Mouse IgG (H+L) Highly Cross-Adsorbed Secondary Antibody, Alexa Fluor Plus 488
596 (Invitrogen, A32723) were diluted to 10 µg/mL.

597

598 **Microscopy and quantification of fluorescent foci**

599

600 Bright-field images and DAPI-stained meiotic chromosomes were pictured using a M-Shot
601 ML31 microscope equipped with a MS60 camera. Aniline blue staining of meiotic cell walls,
602 and immunolocalization of α -tubulin and MR-related proteins were analyzed on an Olympus
603 IX83 inverted fluorescence microscope equipped with a X-Cite lamp and a Prime BSI
604 camera. Image processing and quantification of fluorescent foci were conducted as previously
605 reported (Ning et al., 2021). Briefly, images of DAPI-stained chromosome signals and RFP-
606 channeled protein foci signals were merged, and only the foci merged onto chromosomes
607 were considered the specific foci to targeted proteins, and were counted manually using the
608 Image J count tool.

609

610 **Statistical analysis**

611

612 To analyze the significant difference of orcein-stained tetrad stage meiocytes, meiotic
613 spreading phenotypes, γ H2A.X, DMC1 and HEI10 foci counts, and ASY1/ASY4
614 configurations under different temperatures, nonparametric and unpaired t test was performed
615 using the software GraphPad Prism (version 8). Correlation analysis was conducted using
616 SPSS (IBM, 22.0, the U.S.). Pearson's correlation was used to determine correlation
617 coefficients. * and ** represent P value < 0.05 and 0.01 , respectively. Figures were produced
618 using the R statistical platform (version 3.6.3) via R studio software (version 1.3.1093), and
619 package ggplot2 (version 3.3.3, Wickham, 2009) was used for visualization. The number of
620 cells and/or the biological replicates used for quantification were indicated in the figures
621 and/or supplemental materials.

622

623 **Supplemental materials**

624

625 Supplemental Figure S1. FISH analysis of somatic cells in autotetraploid Col-0.
626 Supplemental Figure S2. Meiotic cell wall formation in autotetraploid Col-0 stressed by 37°C.
627 Supplemental Figure S3. Immunolocalization of α -tubulin in the *dmc1* mutant.
628 Supplemental Figure S4. Meiotic spreading analysis of meiocytes in autotetraploid rice.
629 Supplemental Figure S5. Meiotic spreading analysis of meiocytes in allotetraploid canola.
630 Supplemental Figure S6. Orcein-staining of PMCs in hexaploid *Triticum aestivum*.
631 Supplemental Figure S7. Immunolocalization of ASY1 and ZYP1 in meiocytes of
632 autotetraploid Col-0 at 5 and 28°C.

633 Supplemental Figure S8. Immunolocalization of ASY1 in meiocytes of autotetraploid Col-0 at
634 37°C.

635 Supplemental Figure S9. Immunolocalization of ASY4 in meiocytes of autotetraploid Col-0 at
636 20°C.

637 Supplemental Figure S10. Quantification of ASY1 and ASY4 configurations in diploid and
638 autotetraploid Col-0 stressed by 37°C.

639 Supplemental Figure S11. Immunolocalization of ASY1 and ASY4 in meiocytes of
640 autotetraploid Col-0 at 20°C.

641 Supplemental Table S1. Quantification of pachytene stage meiocytes in autotetraploid Col-0.

642 Supplemental Table S2. Quantification of diakinesis stage meiocytes in autotetraploid Col-0.

643 Supplemental Table S3. Quantification of anaphase I stage meiocytes in autotetraploid Col-0.

644 Supplemental Table S4. Quantification of tetrad stage meiocytes in autotetraploid Col-0.

645 Supplemental Table S5. Primers used in the study.

646

647 **Acknowledgement**

648

649 The authors thank Dr. Jing Li (Huazhong Agricultural University), Dr. Detian Cai (Hubei
650 University) and Dr. Chao Yang (Huazhong Agricultural University) for kindly providing the
651 autotetraploid Col-0 seeds, autotetraploid rice and allotetraploid canola samples, respectively.

652 They thank Dr. Yingxiang Wang (Fudan University) for kindly sharing the anti-HEI10 (rabbit)
653 antibody. They appreciate Dr. Andrew Lloyd (IBERS) for critical review and comments on
654 the manuscript prior to submission.

655

656 **Author contribution**

657

658 H.Q.F. and J.Y.Z. performed immunolocalization experiments; Z.M.R. performed statistical
659 analysis and contributed to data interpretation; K.Y. and X.H.Z. contributed to chromosome
660 spreading analysis; C.W. analyzed fluorescent foci; E.I.E. performed FISH experiment;
661 X.H.Z., J.X., C.L.C., P.L. Y.X.C., H.L. and G.H.Y. contributed to data analysis; B.L.
662 conceived and designed the study, analyzed data, wrote, and edited the manuscript.

663

664 **Funding**

665

666 This work was supported by National Natural Science Foundation of China (32000245 to
667 B.L.), Hubei Provincial Natural Science Foundation of China (2020CFB159 to B.L.),
668 Fundamental Research Funds for the Central Universities, South-Central University for
669 Nationalities (CZY20001 to B.L.), Fundamental Research Funds for the Central Universities,
670 South-Central University for Nationalities (YZZ18007 to B.L.), National Natural Science
671 Foundation of China (31900261 to C.W.), National Natural Science Foundation of China
672 (31270361 to G.H.Y.), Fundamental Research Funds for the Central Universities (CZZ21004
673 to G.H.Y.), and National Natural Science Foundation of China (31971525 to C.L.C.).

674

675 **Interest of conflict**

676

677 All the authors declared that there is no conflict of interest in this work.

678

679

Parsed Citations

Adams, K.L., and Wendel, J.F. (2005). Novel patterns of gene expression in polyploid plants. *Trends Genet* 21, 539-543.

Google Scholar: [Author Only Title Only Author and Title](#)

Allario, T., BRUMOS, J., COLMENERO-FLORES, J.M., IGLESIAS, D.J., PINA, J.A., NAVARRO, L., TALON, M., OLLITRAULT, P., and MORILLON, R. (2013). Tetraploid Rangpur lime rootstock increases drought tolerance via enhanced constitutive root abscisic acid production. *Plant Cell and Environment* 36, 856-868.

Google Scholar: [Author Only Title Only Author and Title](#)

Armstrong, S.J., Caryl, A.P., Jones, G.H., and Franklin, F.C. (2002). *Asy1*, a protein required for meiotic chromosome synapsis, localizes to axis-associated chromatin in *Arabidopsis* and *Brassica*. *J Cell Sci* 115, 3645-3655.

Google Scholar: [Author Only Title Only Author and Title](#)

Bai, X., Peirson, B.N., Dong, F., Xue, C., and Makaroff, C.A. (1999). Isolation and Characterization of *SYN1*, a *RAD21*-like Gene Essential for Meiosis in *Arabidopsis*. *Plant Cell* 11, 417-430.

Google Scholar: [Author Only Title Only Author and Title](#)

Barakate, A., Higgins, J.D., Vivera, S., Stephens, J., Perry, R.M., Ramsay, L., Colas, I., Oakey, H., Waugh, R., Franklin, F.C., Armstrong, S.J., and Halpin, C. (2014). The synaptonemal complex protein *ZYP1* is required for imposition of meiotic crossovers in barley. *Plant Cell* 26, 729-740.

Google Scholar: [Author Only Title Only Author and Title](#)

Berchowitz, L.E., Francis, K.E., Bey, A.L., and Copenhaver, G.P. (2007). The role of *AtMUS81* in interference-insensitive crossovers in *A. thaliana*. *Plos Genet* 3, e132.

Google Scholar: [Author Only Title Only Author and Title](#)

Bergerat, A., de Massy, B., Gadelle, D., Varoutas, P.-C., Nicolas, A., and Forterre, P. (1997). An atypical topoisomerase II from archaea with implications for meiotic recombination. *Nature* 386, 414-417.

Google Scholar: [Author Only Title Only Author and Title](#)

Bombliès, K., Higgins, J.D., and Yant, L. (2015). Meiosis evolves: adaptation to external and internal environments. *New Phytologist* 208, 306-323.

Google Scholar: [Author Only Title Only Author and Title](#)

Bombliès, K., Jones, G., Franklin, C., Zickler, D., and Kleckner, N. (2016). The challenge of evolving stable polyploidy: could an increase in "crossover interference distance" play a central role? *Chromosoma* 125, 287-300.

Google Scholar: [Author Only Title Only Author and Title](#)

Braz, G.T., Yu, F., Zhao, H., Deng, Z., Birchler, J.A., and Jiang, J. (2021). Preferential meiotic chromosome pairing among homologous chromosomes with cryptic sequence variation in tetraploid maize. *New Phytologist* 229, 3294-3302.

Google Scholar: [Author Only Title Only Author and Title](#)

Bretagnolle, F., and Thompson, J.D. (1995). Gametes with the somatic chromosome number: mechanisms of their formation and role in the evolution of autopolyploid plants. *New Phytologist* 129, 1-22.

Google Scholar: [Author Only Title Only Author and Title](#)

Capilla-Pérez, L., Durand, S., Hurel, A., Lian, Q., Chambon, A., Taochy, C., Solier, V., Grelon, M., and Mercier, R. (2021). The synaptonemal complex imposes crossover interference and heterochiasmy in *Arabidopsis*. *Proc Natl Acad Sci U S A* 118, e2023613118.

Google Scholar: [Author Only Title Only Author and Title](#)

Carballo, J.A., Panizza, S., Serrentino, M.E., Johnson, A.L., Geymonat, M., Borde, V., Klein, F., and Cha, R.S. (2013). Budding yeast *ATM/ATR* control meiotic double-strand break (DSB) levels by down-regulating *Rec114*, an essential component of the DSB-machinery. *Plos Genet* 9, e1003545.

Google Scholar: [Author Only Title Only Author and Title](#)

Chambon, A., West, A., Vezon, D., Horlow, C., De Muyt, A., Chelysheva, L., Ronceret, A., Darbyshire, A., Osman, K., Heckmann, S., Franklin, F.C.H., and Grelon, M. (2018). Identification of *ASYNAPTIC4*, a component of the meiotic chromosome axis. *Plant Physiology* 178, 233-246.

Google Scholar: [Author Only Title Only Author and Title](#)

Chelysheva, L., Grandont, L., Vrielynck, N., Guin, S.I., Mercier, R., and Grelon, M. (2010). An easy protocol for studying chromatin and recombination protein dynamics during *Arabidopsis thaliana* meiosis: immunodetection of cohesins, histones and *MLH1*. *Cytogenetic and Genome Research* 129, 143-153.

Google Scholar: [Author Only Title Only Author and Title](#)

Chelysheva, L., Vezon, D., Chambon, A., Gendrot, G., Pereira, L., Lemhemdi, A., Vrielynck, N., Le Guin, S., Novatchkova, M., and Grelon, M. (2012). The *Arabidopsis* *HEI10* is a new ZMM protein related to *Zip3*. *Plos Genet* 8, e1002799-e1002799.

Google Scholar: [Author Only Title Only Author and Title](#)

Chelysheva, L., Diallo, S., Vezon, D., Gendrot, G., Vrielynck, N., Belcram, K., Rocques, N., Márquez-Lema, A., Bhatt, A.M., Horlow, C., Mercier, R., Mézard, C., and Grelon, M. (2005). *AtREC8* and *AtSCC3* are essential to the monopolar orientation of the kinetochores

during meiosis. *Journal of Cell Science* 118, 4621-4632.

Google Scholar: [Author Only](#) [Title Only](#) [Author and Title](#)

Comai, L. (2005). The advantages and disadvantages of being polyploid. *Nature reviews. Genetics* 6, 836-846.

Google Scholar: [Author Only](#) [Title Only](#) [Author and Title](#)

Da Ines, O., Degroote, F., Goubely, C., Amiard, S., Gallego, M.E., and White, C.I. (2013). Meiotic recombination in *Arabidopsis* is catalysed by DMC1, with RAD51 playing a supporting role. *Plos Genet* 9, e1003787.

Google Scholar: [Author Only](#) [Title Only](#) [Author and Title](#)

Da Ines, O., Michard, R., Fayos, I., Bastianelli, G., Nicolas, A., Guiderdoni, E., White, C., and Sourdille, P. (2020). Bread wheat TaSPO11-1 exhibits evolutionarily conserved function in meiotic recombination across distant plant species. *Plant Journal* 103, 2052-2068.

Google Scholar: [Author Only](#) [Title Only](#) [Author and Title](#)

De Muyl, A., Vezon, D., Gendrot, G., Gallois, J.-L., Stevens, R., and Grelon, M. (2007). AtPRD1 is required for meiotic double strand break formation in *Arabidopsis thaliana*. *EMBO Journal* 26, 4126-4137.

Google Scholar: [Author Only](#) [Title Only](#) [Author and Title](#)

De Storme, N., and Geelen, D. (2011). The *Arabidopsis* mutant jason produces unreduced first division restitution male gametes through a parallel/fused spindle mechanism in meiosis II. *Plant Physiology* 155, 1403-1415.

Google Scholar: [Author Only](#) [Title Only](#) [Author and Title](#)

De Storme, N., and Geelen, D. (2014). The impact of environmental stress on male reproductive development in plants: biological processes and molecular mechanisms. *Plant Cell and Environment* 37, 1-18.

Google Scholar: [Author Only](#) [Title Only](#) [Author and Title](#)

De Storme, N., and Geelen, D. (2020). High temperatures alter cross-over distribution and induce male meiotic restitution in *Arabidopsis thaliana*. *Communications Biology* 3, 187.

Google Scholar: [Author Only](#) [Title Only](#) [Author and Title](#)

De Storme, N., Copenhaver, G.P., and Geelen, D. (2012). Production of diploid male gametes in *Arabidopsis* by cold-induced destabilization of postmeiotic radial microtubule arrays. *Plant Physiology* 160, 1808-1826.

Google Scholar: [Author Only](#) [Title Only](#) [Author and Title](#)

Del Pozo, J.C., and Ramirez-Parra, E. (2015). Whole genome duplications in plants: an overview from *Arabidopsis*. *Journal of Experimental Botany* 66, 6991-7003.

Google Scholar: [Author Only](#) [Title Only](#) [Author and Title](#)

Draeger, T., and Moore, G. (2017). Short periods of high temperature during meiosis prevent normal meiotic progression and reduce grain number in hexaploid wheat (*Triticum aestivum* L.). *Theoretical and Applied Genetics* 130, 1785-1800.

Google Scholar: [Author Only](#) [Title Only](#) [Author and Title](#)

Dubcovsky, J., and Dvorak, J. (2007). Genome plasticity a key factor in the success of polyploid wheat under domestication. *Science* 316, 1862-1866.

Google Scholar: [Author Only](#) [Title Only](#) [Author and Title](#)

El Baidouri, M., Murat, F., Veyssiere, M., Molinier, M., Flores, R., Burlot, L., Alaux, M., Quesneville, H., Pont, C., and Salse, J. (2017). Reconciling the evolutionary origin of bread wheat (*Triticum aestivum*). *New Phytologist* 213, 1477-1486.

Google Scholar: [Author Only](#) [Title Only](#) [Author and Title](#)

Ferdous, M., Higgins, J.D., Osman, K., Lambing, C., Roitinger, E., Mechtler, K., Armstrong, S.J., Perry, R., Pradillo, M., Cuñado, N., and Franklin, F.C.H. (2012). Inter-homolog crossing-over and synapsis in *Arabidopsis* meiosis are dependent on the chromosome axis protein ATASY3. *Plos Genet* 8, e1002507-e1002507.

Google Scholar: [Author Only](#) [Title Only](#) [Author and Title](#)

France, M.G., Enderle, J., Röhrig, S., Puchta, H., Franklin, F.C.H., and Higgins, J.D. (2021). ZYP1 is required for obligate cross-over formation and cross-over interference in *Arabidopsis*. *Proc Natl Acad Sci U S A* 118.

Google Scholar: [Author Only](#) [Title Only](#) [Author and Title](#)

Gan, L., Huang, B., Song, Z., Zhang, Y., Zhang, Y., Chen, S., Tong, L., Wei, Z., Yu, L., Luo, X., Zhang, X., Cai, D., and He, Y. (2021). Unique glutelin expression patterns and seed endosperm structure facilitate glutelin accumulation in polyploid rice seed. *Rice* 14, 61.

Google Scholar: [Author Only](#) [Title Only](#) [Author and Title](#)

Garcia, V., Gray, S., Allison, R.M., Cooper, T.J., and Neale, M.J. (2015). Tel1ATM-mediated interference suppresses clustered meiotic double-strand-break formation. *Nature* 520, 114-118.

Google Scholar: [Author Only](#) [Title Only](#) [Author and Title](#)

Grandont, L., Cuñado, N., Coriton, O., Huteau, V., Eber, F., Chèvre, A.M., Grelon, M., Chelysheva, L., and Jenczewski, E. (2014). Homoeologous chromosome sorting and progression of meiotic recombination in *Brassica napus*: ploidy does matter! *Plant Cell* 26, 1448-1463.

Google Scholar: [Author Only](#) [Title Only](#) [Author and Title](#)

Grelon, M., Vezon, D., Gendrot, G., and Pelletier, G. (2001). AtSPO11-1 is necessary for efficient meiotic recombination in plants. *The EMBO journal* 20, 589-600.

Google Scholar: [Author Only](#) [Title Only](#) [Author and Title](#)

Hartung, F., Wurz-Wildersinn, R., Fuchs, J., Schubert, I., Suer, S., and Puchta, H. (2007). The catalytically active tyrosine residues of both SPO11-1 and SPO11-2 are required for meiotic double-strand break induction in *Arabidopsis*. *Plant Cell* 19, 3090-3099.

Google Scholar: [Author Only](#) [Title Only](#) [Author and Title](#)

Henry, I.M., Dilkes, B.P., Tyagi, A., Gao, J., Christensen, B., and Comai, L. (2014). The BOY NAMED SUE quantitative trait locus confers increased meiotic stability to an adapted natural allopolyploid of *Arabidopsis*. *Plant Cell* 26, 181-194.

Google Scholar: [Author Only](#) [Title Only](#) [Author and Title](#)

Higgins, J.D., Armstrong, S.J., Franklin, F.C.H., and Jones, G.H. (2004). The *Arabidopsis* MutS homolog AtMSH4 functions at an early step in recombination: evidence for two classes of recombination in *Arabidopsis*. *Genes & development* 18, 2557-2570.

Google Scholar: [Author Only](#) [Title Only](#) [Author and Title](#)

Higgins, J.D., Sanchez-Moran, E., Armstrong, S.J., Jones, G.H., and Franklin, F.C. (2005). The *Arabidopsis* synaptonemal complex protein ZYP1 is required for chromosome synapsis and normal fidelity of crossing over. *Genes & development* 19, 2488-2500.

Google Scholar: [Author Only](#) [Title Only](#) [Author and Title](#)

Hollingsworth, N.M., and Brill, S.J. (2004). The Mus81 solution to resolution: generating meiotic crossovers without Holliday junctions. *Genes & development* 18, 117-125.

Google Scholar: [Author Only](#) [Title Only](#) [Author and Title](#)

Jackson, S., and Chen, Z.J. (2010). Genomic and expression plasticity of polyploidy. *Current Opinion in Plant Biology* 13, 153-159.

Google Scholar: [Author Only](#) [Title Only](#) [Author and Title](#)

Joyce, E.F., Pedersen, M., Tiong, S., White-Brown, S.K., Paul, A., Campbell, S.D., and McKim, K.S. (2011). *Drosophila* ATM and ATR have distinct activities in the regulation of meiotic DNA damage and repair. *Journal of Cell Biology* 195, 359-367.

Google Scholar: [Author Only](#) [Title Only](#) [Author and Title](#)

Klimyuk, V.I., and Jones, J.D.G. (1997). AtDMC1, the *Arabidopsis* homologue of the yeast DMC1 gene: characterization, transposon-induced allelic variation and meiosis-associated expression. *Plant Journal* 11, 1-14.

Google Scholar: [Author Only](#) [Title Only](#) [Author and Title](#)

Kobayashi, W., Liu, E., Ishii, H., Matsunaga, S., Schlogelhofer, P., and Kurumizaka, H. (2019). Homologous pairing activities of *Arabidopsis thaliana* RAD51 and DMC1. *Journal of biochemistry* 165, 289-295.

Google Scholar: [Author Only](#) [Title Only](#) [Author and Title](#)

Kurzbauer, M.-T., Janisiw, M.P., Paulin, L.F., Prusén Mota, I., Tomanov, K., Krsicka, O., Haeseler, Av., Schubert, V., and Schlögelhofer, P. (2021). ATM controls meiotic DNA double-strand break formation and recombination and affects synaptonemal complex organization in plants. *Plant Cell*.

Google Scholar: [Author Only](#) [Title Only](#) [Author and Title](#)

Kurzbauer, M.T., Uanschou, C., Chen, D., and Schlogelhofer, P. (2012). The recombinases DMC1 and RAD51 are functionally and spatially separated during meiosis in *Arabidopsis*. *Plant Cell* 24, 2058-2070.

Google Scholar: [Author Only](#) [Title Only](#) [Author and Title](#)

Lambing, C., Kuo, P.C., Tock, A.J., Topp, S.D., and Henderson, I.R. (2020a). ASY1 acts as a dosage-dependent antagonist of telomere-led recombination and mediates crossover interference in *Arabidopsis*. *Proc Natl Acad Sci U S A* 117, 13647-13658.

Google Scholar: [Author Only](#) [Title Only](#) [Author and Title](#)

Lambing, C., Tock, A.J., Topp, S.D., Choi, K., Kuo, P.C., Zhao, X., Osman, K., Higgins, J.D., Franklin, F.C.H., and Henderson, I.R. (2020b). Interacting genomic landscapes of REC8-cohesin, chromatin, and meiotic recombination in *Arabidopsis*. *Plant Cell* 32, 1218-1239.

Google Scholar: [Author Only](#) [Title Only](#) [Author and Title](#)

Lange, J., Pan, J., Cole, F., Thelen, M.P., Jasin, M., and Keeney, S. (2011). ATM controls meiotic double-strand-break formation. *Nature* 479, 237-240.

Google Scholar: [Author Only](#) [Title Only](#) [Author and Title](#)

Lei, X., Ning, Y., Eid Elesawi, I., Yang, K., Chen, C., Wang, C., and Liu, B. (2020). Heat stress interferes with chromosome segregation and cytokinesis during male meiosis in *Arabidopsis thaliana*. *Plant Signaling & Behavior* 15, 1746985.

Google Scholar: [Author Only](#) [Title Only](#) [Author and Title](#)

Leitch, A.R., and Leitch, I.J. (2008). Genomic plasticity and the diversity of polyploid plants. *Science* 320, 481-483.

Google Scholar: [Author Only](#) [Title Only](#) [Author and Title](#)

Li, W., Chen, C., Markmann-Mulisch, U., Timofejeva, L., Schmelzer, E., Ma, H., and Reiss, B. (2004). The *Arabidopsis* AtRAD51 gene is dispensable for vegetative development but required for meiosis. *Proc Natl Acad Sci U S A* 101, 10596-10601.

Google Scholar: [Author Only](#) [Title Only](#) [Author and Title](#)

Li, Z., McKibben, M.T.W., Finch, G.S., Blischak, P.D., Sutherland, B.L., and Barker, M.S. (2021). Patterns and processes of diploidization in land plants. *Annual Review of Plant Biology* 72, 387-410.

Google Scholar: [Author Only](#) [Title Only](#) [Author and Title](#)

Liu, B., De Storme, N., and Geelen, D. (2017). Cold interferes with male meiotic cytokinesis in *Arabidopsis thaliana* independently of the

AHK2/3-AHP2/3/5 cytokinin signaling module. Cell Biology International 41, 879-889.

Google Scholar: [Author Only Title Only Author and Title](#)

Liu, B., De Storme, N., and Geelen, D. (2018). Cold-induced male meiotic restitution in *Arabidopsis thaliana* is not mediated by GA-DELLA signaling. Frontiers in Plant Science 9, 91.

Google Scholar: [Author Only Title Only Author and Title](#)

Liu, B., Mo, W.J., Zhang, D., De Storme, N., and Geelen, D. (2019). Cold influences male reproductive development in plants: a hazard to fertility, but a window for evolution. Plant Cell Physiology 60, 7-18.

Google Scholar: [Author Only Title Only Author and Title](#)

Lloyd, A., and Bomblies, K. (2016). Meiosis in autopolyploid and allopolyploid *Arabidopsis*. Current Opinion in Plant Biology 30, 116-122.

Google Scholar: [Author Only Title Only Author and Title](#)

Lloyd, A., Morgan, C., H. Franklin, F.C., and Bomblies, K. (2018). Plasticity of Meiotic Recombination Rates in Response to Temperature in *Arabidopsis*. Genetics 208, 1409-1420.

Google Scholar: [Author Only Title Only Author and Title](#)

Lohani, N., Singh, M.B., and Bhalla, P.L. (2019). High temperature susceptibility of sexual reproduction in crop plants. Journal of Experimental Botany 71, 555-568.

Google Scholar: [Author Only Title Only Author and Title](#)

Loidl, J. (1989). Effects of elevated temperature on meiotic chromosome synapsis in *Allium ursinum*. Chromosoma 97, 449-458.

Google Scholar: [Author Only Title Only Author and Title](#)

Lourkisti, R., Froelicher, Y., Herbette, S., Morillon, R., Tomi, F., Gibernau, M., Giannettini, J., Berti, L., and Santini, J. (2020). Triploid citrus genotypes have a better tolerance to natural chilling conditions of photosynthetic capacities and specific leaf volatile organic compounds. Frontiers in Plant Science 11.

Google Scholar: [Author Only Title Only Author and Title](#)

Lu, K., Wei, L., Li, X., Wang, Y., Wu, J., Liu, M., Zhang, C., Chen, Z., Xiao, Z., Jian, H., Cheng, F., Zhang, K., Du, H., Cheng, X., Qu, C., Qian, W., Liu, L., Wang, R., Zou, Q., Ying, J., Xu, X., Mei, J., Liang, Y., Chai, Y.R., Tang, Z., Wan, H., Ni, Y., He, Y., Lin, N., Fan, Y., Sun, W., Li, N.N., Zhou, G., Zheng, H., Wang, X., Paterson, A.H., and Li, J. (2019). Whole-genome resequencing reveals *Brassica napus* origin and genetic loci involved in its improvement. Nat Commun 10, 1154.

Google Scholar: [Author Only Title Only Author and Title](#)

Mai, Y., Li, H., Suo, Y., Fu, J., Sun, P., Han, W., Diao, S., and Li, F. (2019). High temperature treatment generates unreduced pollen in persimmon (*Diospyros kaki* Thunb.). Scientia Horticulturae 258, 108774.

Google Scholar: [Author Only Title Only Author and Title](#)

Modliszewski, J.L., Wang, H., Albright, A.R., Lewis, S.M., Bennett, A.R., Huang, J., Ma, H., Wang, Y., and Copenhaver, G.P. (2018). Elevated temperature increases meiotic crossover frequency via the interfering (Type I) pathway in *Arabidopsis thaliana*. Plos Genet 14, e1007384.

Google Scholar: [Author Only Title Only Author and Title](#)

Mohibullah, N., and Keeney, S. (2017). Numerical and spatial patterning of yeast meiotic DNA breaks by Tel1. Genome research 27, 278-288.

Google Scholar: [Author Only Title Only Author and Title](#)

Morgan, C., Zhang, H., Henry, C.E., Franklin, F.C.H., and Bomblies, K. (2020). Derived alleles of two axis proteins affect meiotic traits in autotetraploid *Arabidopsis arenosa*. Proc Natl Acad Sci U S A 117, 8980-8988.

Google Scholar: [Author Only Title Only Author and Title](#)

Morgan, C.H., Zhang, H., and Bomblies, K. (2017). Are the effects of elevated temperature on meiotic recombination and thermotolerance linked via the axis and synaptonemal complex? Philosophical transactions of the Royal Society of London. Series B, Biological sciences 372, 20160470.

Google Scholar: [Author Only Title Only Author and Title](#)

Ning, Y., Liu, Q., Wang, C., Qin, E., Wu, Z., Wang, M., Yang, K., Elesawi, I.E., Chen, C., Liu, H., Qin, R., and Liu, B. (2021). Heat stress interferes with formation of double-strand breaks and homolog synapsis. Plant Physiology 185, 1783-1797.

Google Scholar: [Author Only Title Only Author and Title](#)

Osman, K., Yang, J., Roitinger, E., Lambing, C., Heckmann, S., Howell, E., Cuacos, M., Imre, R., Durnberger, G., Mechtler, K., Armstrong, S., and Franklin, F.C.H. (2018). Affinity proteomics reveals extensive phosphorylation of the *Brassica* chromosome axis protein ASY1 and a network of associated proteins at prophase I of meiosis. Plant Journal 93, 17-33.

Google Scholar: [Author Only Title Only Author and Title](#)

Otto, S.P. (2007). The evolutionary consequences of polyploidy. Cell 131, 452-462.

Google Scholar: [Author Only Title Only Author and Title](#)

Parisod, C., Holderegger, R., and Brochmann, C. (2010). Evolutionary consequences of autopolyploidy. New Phytologist 186, 5-17.

Google Scholar: [Author Only Title Only Author and Title](#)

Paull, T.T. (2015). Mechanisms of ATM activation. Annual review of biochemistry 84, 711-738.

Google Scholar: [Author Only](#) [Title Only](#) [Author and Title](#)

Pohl, T.J., and Nickoloff, J.A. (2008). Rad51-independent interchromosomal double-strand break repair by gene conversion requires Rad52 but not Rad55, Rad57, or Dmc1. *Mol Cell Biol* 28, 897-906.

Google Scholar: [Author Only](#) [Title Only](#) [Author and Title](#)

Ramsey, J., and Schemske, D.W. (1998). Pathways, mechanisms, and rates of polyploid formation in flowering plants. *Annual Review of Ecology and Systematics* 29, 467-501.

Google Scholar: [Author Only](#) [Title Only](#) [Author and Title](#)

Ramsey, J., and Schemske, D.W. (2002). Neopolyploidy in flowering plants. *Annual Review of Ecology and Systematics* 33, 589-639.

Google Scholar: [Author Only](#) [Title Only](#) [Author and Title](#)

Rao, S., Tian, Y., Xia, X., Li, Y., and Chen, J. (2020). Chromosome doubling mediates superior drought tolerance in *Lycium ruthenicum* via abscisic acid signaling. *Horticulture research* 7, 40.

Google Scholar: [Author Only](#) [Title Only](#) [Author and Title](#)

Ren, R., Wang, H.F., Guo, C.C., Zhang, N., Zeng, L.P., Chen, Y.M., Ma, H., and Qi, J. (2018). Widespread whole genome duplications contribute to genome complexity and species diversity in angiosperms. *Molecular Plant* 11, 414-428.

Google Scholar: [Author Only](#) [Title Only](#) [Author and Title](#)

Sanchez-Moran, E., Santos, J.L., Jones, G.H., and Franklin, F.C. (2007). ASY1 mediates AtDMC1-dependent interhomolog recombination during meiosis in *Arabidopsis*. *Genes & development* 21, 2220-2233.

Google Scholar: [Author Only](#) [Title Only](#) [Author and Title](#)

Santos, J.L., Alfaro, D., Sanchez-Moran, E., Armstrong, S.J., Franklin, F.C.H., and Jones, G.H. (2003). Partial diploidization of meiosis in autotetraploid *Arabidopsis thaliana*. *Genetics* 165, 1533-1540.

Google Scholar: [Author Only](#) [Title Only](#) [Author and Title](#)

Schindfessel, C., Drozdowska, Z., De Mooij, L., and Geelen, D. (2021). Loss of obligate crossovers, defective cytokinesis and male sterility in barley caused by short-term heat stress. *Plant Reproduction*.

Google Scholar: [Author Only](#) [Title Only](#) [Author and Title](#)

Seear, P.J., France, M.G., Gregory, C.L., Heavens, D., Schnickl, R., Yant, L., and Higgins, J.D. (2020). A novel allele of ASY3 is associated with greater meiotic stability in autotetraploid *Arabidopsis lyrata*. *Plos Genet* 16, e1008900-e1008900.

Google Scholar: [Author Only](#) [Title Only](#) [Author and Title](#)

Shi, W., Ji, J., Xue, Z., Zhang, F., Miao, Y., Yang, H., Tang, D., Du, G., Li, Y., Shen, Y., and Cheng, Z. (2021). PRD1, a homologous recombination initiation factor, is involved in spindle assembly in rice meiosis. *New Phytologist* 230, 585-600.

Google Scholar: [Author Only](#) [Title Only](#) [Author and Title](#)

Shi, W., Tang, D., Shen, Y., Xue, Z., Zhang, F., Zhang, C., Ren, L., Liu, C., Du, G., Li, Y., Yan, C., and Cheng, Z. (2019). OsHOP2 regulates the maturation of crossovers by promoting homologous pairing and synapsis in rice meiosis. *New Phytologist* 222, 805-819.

Google Scholar: [Author Only](#) [Title Only](#) [Author and Title](#)

Singh, G., Da Ines, O., Gallego, M.E., and White, C.I. (2017). Analysis of the impact of the absence of RAD51 strand exchange activity in *Arabidopsis* meiosis. *PLoS One* 12, e0183006.

Google Scholar: [Author Only](#) [Title Only](#) [Author and Title](#)

Soltis, P.S., and Soltis, D.E. (2009). The role of hybridization in plant speciation. *Annu Rev Plant Biol* 60, 561-588.

Google Scholar: [Author Only](#) [Title Only](#) [Author and Title](#)

Soltis, P.S., Marchant, D.B., Van de Peer, Y., and Soltis, D.E. (2015). Polyploidy and genome evolution in plants. *Curr Opin Genet Dev* 35, 119-125.

Google Scholar: [Author Only](#) [Title Only](#) [Author and Title](#)

Stacey, N.J., Kuromori, T., Azumi, Y., Roberts, G., Breuer, C., Wada, T., Maxwell, A., Roberts, K., and Sugimoto-Shirasu, K. (2006). *Arabidopsis* SPO11-2 functions with SPO11-1 in meiotic recombination. *Plant Journal* 48, 206-216.

Google Scholar: [Author Only](#) [Title Only](#) [Author and Title](#)

Stift, M., Berenos, C., Kuperus, P., and van Tienderen, P.H. (2008). Segregation models for disomic, tetrasomic and intermediate inheritance in tetraploids: a general procedure applied to rorippa (Yellow Cress) microsatellite data. *Genetics* 179, 2113-2123.

Google Scholar: [Author Only](#) [Title Only](#) [Author and Title](#)

Su, H., Cheng, Z., Huang, J., Lin, J., Copenhaver, G.P., Ma, H., and Wang, Y. (2017). *Arabidopsis* RAD51, RAD51C and XRCC3 proteins form a complex and facilitate RAD51 localization on chromosomes for meiotic recombination. *Plos Genet* 13, e1006827.

Google Scholar: [Author Only](#) [Title Only](#) [Author and Title](#)

Svačina, R., Sourdille, P., Kopecký, D., and Bartoš, J. (2020). Chromosome pairing in polyploid grasses. *Frontiers in Plant Science* 11, 1056.

Google Scholar: [Author Only](#) [Title Only](#) [Author and Title](#)

Tang, Z., Zhang, L., Yang, D., Zhao, C., and Zheng, Y. (2011). Cold stress contributes to aberrant cytokinesis during male meiosis I in a wheat thermosensitive genic male sterile line. *Plant Cell and Environment* 34, 389-405.

Google Scholar: [Author Only](#) [Title Only](#) [Author and Title](#)

te Beest, M., Le Roux, J.J., Richardson, D.M., Brysting, A.K., Suda, J., Kubesová, M., and Pysek, P. (2012). The more the better? The role of polyploidy in facilitating plant invasions. *Annals of botany* 109, 19-45.

Google Scholar: [Author Only](#) [Title Only](#) [Author and Title](#)

Van de Peer, Y., Ashman, T.-L., Soltis, P.S., and Soltis, D.E. (2020). Polyploidy: an evolutionary and ecological force in stressful times. *Plant Cell* 33, 11-26.

Google Scholar: [Author Only](#) [Title Only](#) [Author and Title](#)

Wang, J., Li, D., Shang, F., and Kang, X. (2017). High temperature-induced production of unreduced pollen and its cytological effects in *Populus*. *Sci Rep-Uk* 7, 5281.

Google Scholar: [Author Only](#) [Title Only](#) [Author and Title](#)

Wang, K., Wang, M., Tang, D., Shen, Y., Miao, C., Hu, Q., Lu, T., and Cheng, Z. (2012). The role of rice HEI10 in the formation of meiotic crossovers. *Plos Genet* 8, e1002809-e1002809.

Google Scholar: [Author Only](#) [Title Only](#) [Author and Title](#)

Wang, M., Wang, K., Tang, D., Wei, C., Li, M., Shen, Y., Chi, Z., Gu, M., and Cheng, Z. (2010). The central element protein ZEP1 of the synaptonemal complex regulates the number of crossovers during meiosis in rice. *Plant Cell* 22, 417-430.

Google Scholar: [Author Only](#) [Title Only](#) [Author and Title](#)

Wang, Y., and Copenhaver, G.P. (2018). Meiotic recombination: mixing it up in plants. *Annual Review of Plant Biology* 69, 577-609.

Google Scholar: [Author Only](#) [Title Only](#) [Author and Title](#)

Wang, Y., Cheng, Z., Lu, P., Timofejeva, L., and Ma, H. (2014). Molecular cell biology of male meiotic chromosomes and isolation of male meiocytes in *Arabidopsis thaliana*. *Methods in molecular biology (Clifton, N.J.)* 1110, 217-230.

Google Scholar: [Author Only](#) [Title Only](#) [Author and Title](#)

Weitz, A.P., Dukic, M., Zeitler, L., and Bomblies, K. (2021). Male meiotic recombination rate varies with seasonal temperature fluctuations in wild populations of autotetraploid *Arabidopsis arenosa*. *Molecular Ecology* 00, 1-12.

Google Scholar: [Author Only](#) [Title Only](#) [Author and Title](#)

Wu, S., Han, B., and Jiao, Y. (2020). Genetic contribution of paleopolyploidy to adaptive evolution in angiosperms. *Molecular Plant* 13, 59-71.

Google Scholar: [Author Only](#) [Title Only](#) [Author and Title](#)

Xue, M., Wang, J., Jiang, L., Wang, M., Wolfe, S., Pawlowski, W.P., Wang, Y., and He, Y. (2018). The number of meiotic double-strand breaks influences crossover distribution in *Arabidopsis*. *Plant Cell* 30, 2628-2638.

Google Scholar: [Author Only](#) [Title Only](#) [Author and Title](#)

Xue, Z., Liu, C., Shi, W., Miao, Y., Shen, Y., Tang, D., Li, Y., You, A., Xu, Y., Chong, K., and Cheng, Z. (2019). OsMTPMB is required for meiotic bipolar spindle assembly. *Proc Natl Acad Sci U S A* 116, 15967-15972.

Google Scholar: [Author Only](#) [Title Only](#) [Author and Title](#)

Yant, L., Hollister, J.D., Wright, K.M., Arnold, B.J., Higgins, J.D., Franklin, F.C.H., and Bomblies, K. (2013). Meiotic adaptation to genome duplication in *Arabidopsis arenosa*. *Current Biology* 23, 2151-2156.

Google Scholar: [Author Only](#) [Title Only](#) [Author and Title](#)

Yao, Y., Li, X., Chen, W., Liu, H., Mi, L., Ren, D., Mo, A., and Lu, P. (2020). ATM Promotes RAD51-Mediated Meiotic DSB Repair by Inter-Sister-Chromatid Recombination in *Arabidopsis*. *Frontiers in Plant Science* 11, 839.

Google Scholar: [Author Only](#) [Title Only](#) [Author and Title](#)

Zhang, L., Kim, K.P., Kleckner, N.E., and Storlazzi, A. (2011). Meiotic double-strand breaks occur once per pair of (sister) chromatids and, via Mec1/ATR and Tel1/ATM, once per quartet of chromatids. *Proc Natl Acad Sci U S A* 108, 20036-20041.

Google Scholar: [Author Only](#) [Title Only](#) [Author and Title](#)

Zickler, D., and Kleckner, N. (1999). Meiotic chromosomes: integrating structure and function. *Annual review of genetics* 33, 603-754.

Google Scholar: [Author Only](#) [Title Only](#) [Author and Title](#)